Article

Benzylideneacetone Derivatives Inhibit Osteoclastogenesis and Activate Osteoblastogenesis Independently Based on Specific Structure–Activity Relationship

Triveni Pativada, Myung Hwan Kim, Jung-Hun Lee, Seong Su Hong, Chun Whan Choi, Yun-Hyeok Choi, Woo Jung Kim, Da-Woon Song, Serk In Park, Eun Jung Lee, Bo-Yeon Seo, Hankyeom Kim, Hong Kyu Kim, Kee-Ho Lee, Sung k Ahn, Jin-Mo Ku, and Gil Hong Park

Just Accepted

Benzylideneacetone Derivatives Inhibit Osteoclastogenesis and Activate Osteoblastogenesis Independently Based on Specific Structure–Activity Relationship

Triveni Pativada,[†#] Myung Hwan Kim,[†#] Jung-Hun Lee,[‡#] Seong Su Hong,[‡] Chun Whan Choi,[‡] Yun-Hyeok Choi,[‡] Woo Jung Kim,[‡] Da-Woon Song,[‡] Serk In Park,[†] Eun Jung Lee,[†] Bo-Yeon Seo,[†] Hankyeom Kim,[§] Hong Kyu Kim,[‖] Kee Ho Lee,[⊥] Sung K Ahn,[▽] Jin-Mo Ku,[*‡] and Gil Hong Park[*†]

[†]Department of Biochemistry and Molecular Biology, College of Medicine, Korea Molecular Medicine and Nutrition Research Institute, Korea University, Seoul 02841, Korea

[‡]Bio-Center, Gyeonggido Business & Science Accelerator, Suwon 16229, Korea

[§]Department of Pathology, Korea University Guro Hospital, Seoul 08308, Korea

[‖]Department of Surgery, Seoul National University Hospital, Seoul 03080, Korea

[⊥]Division of Radiation Cancer Research, Korea Institute of Radiological and Biomedical Sciences, Seoul 01812, Korea

[▽]Statistics, Department of Finance and Management Science, College of Business, Washington State University, Pullman, WA 99164-4746, United States

ABSTRACT: (*E*)-3,4-Dihydroxybenzylideneacetone (compound **1**), inhibited receptor activator of NF-kB ligand-induced osteoclastogenesis of C57BL/6 bone marrow

monocyte/macrophages with IC_{50} of 7.8 µM (IC_{50} of alendronate, 3.7 µM), while stimulating the differentiation of MC3T3-E1 osteoblastic cells, accompanied by the induction of Runt-related transcription factor 2, alkaline phosphatase and osteocalcin. (*E*)-4-(3-Hydroxy-4-methoxyphenyl)-3-buten-2-one (compound **2c**) showed a dramatically increased osteoclast-inhibitory potency with IC_{50} of 0.11 µM, while sustaining osteoblast-stimulatory activity. (*E*)-4-(4-Hydroxy-3-methoxyphenyl)-3-buten-2-one (compound **2g**) stimulated alkaline phosphatase production 2 folds at 50 µM without changing osteoclast-inhibitory activity, compared with compound **1**. Oral administration of compounds **1**, **2c**, and **2g** prevented ovariectomy-induced osteoporosis in ddY mice to a degree proportional to their osteoclastogenesis-inhibitory potencies. The administration of 1 mg/kg/d compound **2c** ameliorated histomorphometry of osteoporotic bone to a degree comparable with 10 mg/kg/d alendronate. Conclusively, the *in vitro* capacity of a few benzylideneacetone derivatives to inhibit osteoclastogenesis supported by independent osteoblastogenesis activation was convincingly reflected in *in vivo* management of osteoporosis, suggesting a potential novel therapeutics for osteopenic diseases.

INTRODUCTION

Bone is a dynamic organ in which the existing matrix is continually resorbed by osteoclasts of hematopoietic origin, and replaced by osteoblasts of mesenchymal origin.[1] Excessive bone resorption by osteoclasts aggravates osteopenic diseases such as osteoporosis, thereby increasing the frequency of arthralgia and fracture. Continuous bone resorption due to abnormal osteoclastic activity and subsequent abnormal replacement of matrix by osteoblasts leads to bone deformities which increases vulnerability to fractures; a condition known as Paget's disease of bone.[2] Currently, the most widely used clinical therapeutics for osteopenic

diseases include osteoclast-inhibitory agents such as bisphosphonates, including alendronate,[3] and anabolics represented by parathyroid hormone (PTH) regimens, which act to enhance osteoblast activity.[4] Interactions between bone marrow and cancer cells, results in increased bone turnover that facilitates cancer bone metastasis.[5] Among many cell populations constituting the bone marrow microenvironment, osteoclasts are key players in the development of osteolytic lesions for cancer metastasis.[6,7] Zoledronic acid, a bisphosphonate drug which inhibits osteoclastogenesis, preserves the integrity of tumor-bearing bones and increases the survival time of prostate cancer patients.[8] When PTH was administered concurrently with zoledronic acid, there was a remarkable decrease in the incidence of prostate cancer metastasis to the skeleton, suggesting that simultaneously suppressing bone destruction while promoting bone formation resulted in much greater suppression of tumor bone metastasis.[5]

Osteoclasts differentiate from bone marrow monocyte/macrophage lineage cells (BMM) which are under the control of two essential cytokines, macrophage colony-stimulating factor (M-CSF) and receptor activator of NF-kB ligand (RANKL).[9,10] Additionally, signals arising from antibodies such as autoimmune antibodies in rheumatoid arthritis that enhance receptor activator of NF-kB (RANK) signaling, are necessary for complete differentiation of osteoclasts.[11,12] NF-kB activated by RANK in early osteoclastogenesis is one of the crucial transcription factors underlying osteoclastogenesis,[13] which stimulates the induction of nuclear factor of activated T-cell cytoplasmic 1 (NFATc1), a master transcription factor for the terminal differentiation of osteoclasts.[14] Osteoblast-induced bone formation is regulated by various hormones including PTH, growth factors, and cytokines, as well as by nutrition, mechanical loading, and aging.[15-18] Runt-related transcription factor 2 (RUNX2) is an early-stage transcription factor strongly associated with osteoblastic differentiation and calcification.[19] RUNX2 increases bone formation by stimulating the transcription of bone-

forming proteins such as alkaline phosphatase (ALP), an early/intermediate stage marker of osteoblastogenesis, and osteocalcin (OCN), a late-stage osteoblastic differentiation marker. Bone-ALP is an indicator of bone formation,[20] and OCN constitutes a major non-collagenous matrix protein in bone.[21] Homeostasis of bone involves tightly regulated interactions between osteoblasts and osteoclasts, suggesting that osteoblast differentiation promotes osteoclast differentiation.[22] Thus, any modification of osteoclast differentiation by disease or drugs tends to induce parallel changes in osteoblasts, posing challenges for the management of osteopenic diseases.[23,24] However, crosstalk between pathways regulating osteoclastogenesis and osteoblastogenesis for bone homeostasis, have yet to be fully elucidated.

In this study, we have examined the capacity of benzylideneacetone derivatives for their ability to independently promote osteoclastogenic inhibition and osteoblastogenic activation, and determined specific structure-activity relationship (SAR) in an effort to search for key structural determinants of these biological activities with the aim of discovering compounds with increased potency. Compound **1** is a constituent of *Osmunda japonica* rhizome,[25] and is known to inhibit the production of immune mediators such as cytokines (TNF-alpha, interleukin-1β, interleukin-6), NO, and prostaglandin E2 that play crucial roles in the development of rheumatoid arthritis,[26,27] as well as to activate osteoblast differentiation[28] and exert cancer-specific cytotoxicity.[29] *Osmunda regalis* L., a species closely related to *Osmunda japonica*, has been used in Spain for hundreds of years as a highly efficient remedy for treating rheumatoid arthritis and pain, without clinically significant adverse effects.[30] The rhizome of ginger (*Zingiber officinale*) has been used as an herbal drug for the management of osteoporosis in Indian ethnopharmacology as well as food additives,[31] and suppresses RANKL-induced osteoclastogenesis.[32] Compound **2g** is a pungent constituent of ginger, and compound **2c** is its synthetic isomer.[33] The capacities of these compounds to prevent bone loss *in vivo* was investigated in ovariectomy (OVX)-induced osteoporotic mice. Furthermore, we investigated

the effect of compounds **1**, **2c**, and **2g** on the expression of differentiation markers including key transcription factors for the differentiation of osteoclasts and osteoblasts during osteoclastogenesis and osteoblastogenesis.

RESULTS

Synthesis of Novel Benzylideneacetone Derivatives. Derivatives of compound **1** (Figure 1) were designed and synthesized chemically *de novo* for SAR analysis, and isolated with purities higher than 95% (Supporting Information 1). Compound **2g** (CAS; 1080-12-2) is a constituent of ginger.[33] Compounds **2c** (CAS; 22214-39-7)[33] and **2h** (CAS; 1704417-22-0) are synthetic compounds reported previously. The remainder (**2a**, **2b**, **2d**, **2e**, **2f**, **3a**, and **3b**) were novel compounds. Structures of synthesized compounds were identified by analysis of spectral data including MS, 1-D and 2-D NMR (Supporting Information 2).

R[1] = Me, osmundacetone (**1**)   R[2] = H, trans-cinnamic acid   Phenylacetic acid
   OH, caffeic acid   OH, 4-hydroxybenzalacetone

R[3] = OH, homoprotocatechuic acid   R[4] = H, protocatechualehyde
   OMe, homoprotocatechuic acid methyl ester   OH, protocatechuic acid
                                               OMe, protocatechuic acid methyl ester

Neochlorogenic acid   Chlorogenic acid   Alendronic acid

2a, R[5] = Me
2b, R[5] = F
2c, R[5] = OMe
2d, R[5] = OiPr
2e, R[5] = OBn
2f, R[5] = Oallyl

2g, R[6] = OMe
2h, R[6] = F
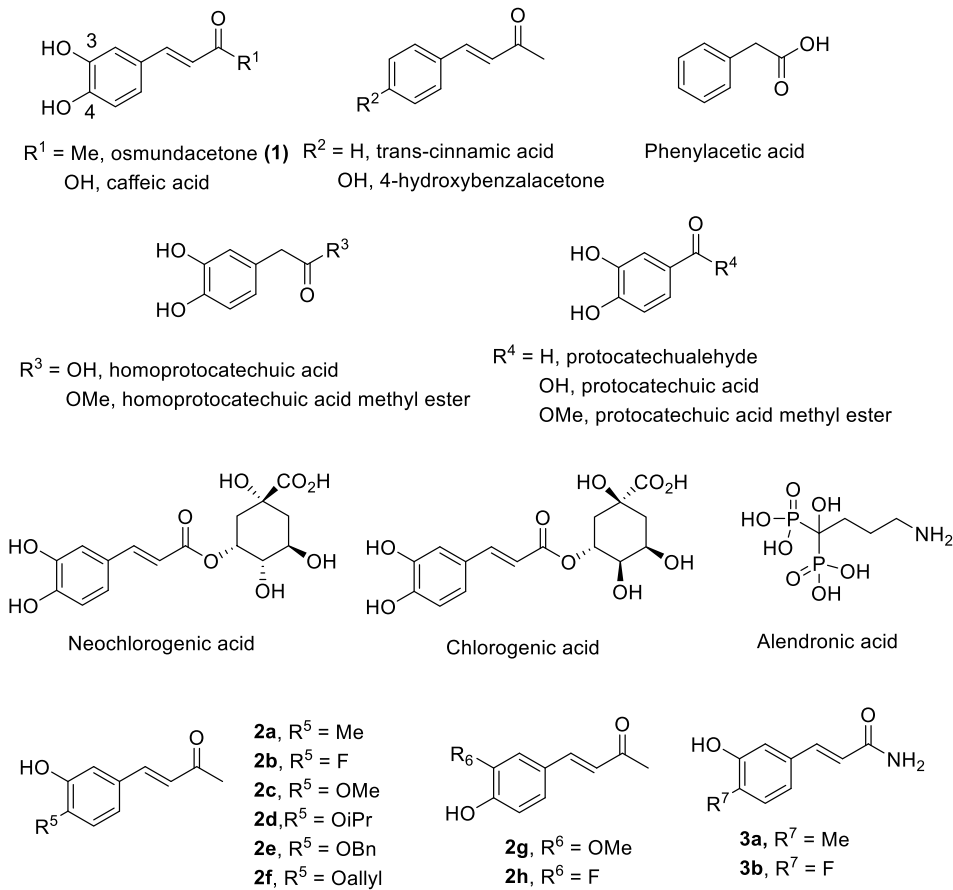
3a, R[7] = Me
3b, R[7] = F

Figure 1. Structures of compound **1** and its structural analogues.

Purity Determination of Compounds 2a−h and 3a, b. For qualitative analysis, an Agilent 1200 series HPLC instrument (Agilent Technologies, Inc. Santa Clara, CA) was used. Analyses were carried out on a Waters TC-C18 reversed-phase analytical column (2.1 × 50 mm, 2 μm) (Waters Co., Milford, MA). The detection wavelength was set at 250 nm. The mobile phase consisted of the solvent A (0.1%, v/v solution of formic acid in water) and solvent B (0.1%, v/v solution of formic acid in acetonitrile), and was subject to gradient elution. As a result, ≥95% purity was confirmed for each compound tested. Purity and NMR data of the synthesized compounds are presented in Supporting Information 1, 2.

Compound 1 Inhibits the Differentiation of Preosteoclasts in a Concentration-Dependent Manner, Independently of Concurrent Proliferation of Co-Existing Preosteoblasts. To evaluate the effect of compound **1** on osteoclast differentiation, we isolated BMM (preosteoclasts) from C57BL/6 mice, and induced osteoclastogenesis in the presence of a range of concentrations of compound **1,** or of alendronate as a reference compound. BMM differentiated into mature multinucleated osteoclasts in 6 d, in the presence of M-CSF and RANKL, and were identified by tartrate-resistant acid phosphatase (TRAP) staining (Figure 2A, Positive control). In contrast, BMM grown in the presence of M-CSF only, failed to differentiate into mature multinucleated osteoclasts (Figure 2A, Negative control). Compound **1** suppressed the proliferation and differentiation of osteoclasts with an IC_{50} of approximately 7.8 μM, and almost completely inhibited osteoclastogenesis at 10 μM (Figure 2A, Compound **1**). Alendronate inhibited osteoclastogenesis with an IC_{50} of approximately 3.7 μM in the same setting (Figure 2A, Alendronate). To determine if compound **1** inhibits the bone resorption function of fully differentiated mature osteoclasts, we performed a bone resorption assay with

mature multinucleated osteoclasts in the presence of compound **1** at the IC_{50} concentration. Under the condition, it suppressed bone resorption of mature osteoclasts up to $59 \pm 10\%$ in 3 d compared to that of untreated mature osteoclasts. Compound **1** inhibited the differentiation of preosteoclasts without inhibiting the proliferation of co-existing preosteoblasts (MC3T3-E1 murine osteoblastic cells), as shown in the compound **1**-treated co-culture of preosteoclasts and preosteoblasts in the presence of differentiation factors for both cell types (Figure 2B, Compound **1**). Preosteoclasts failed to differentiate into mature multinucleated osteoclasts in 6 d, and preosteoblasts continued to proliferate in the presence of 10 μM compound **1**. By contrast, in the absence of compound **1**, both preosteoclasts and preosteoblasts appeared to proliferate and differentiate in the presence of differentiation factors until day 7 after induction (Figure 2B, Positive control). In this setting, differentiated osteoclasts were smaller than those grown in the absence of osteoblasts, which may be attributed to steric hindrance of cell growth, due to the high cell concentrations resulting from co-existence of proliferating preosteoclasts and preosteoblasts. Meanwhile, preosteoclasts and preosteoblasts grown in the presence of M-CSF only, continued to proliferate, but preosteoclasts failed to differentiate into mature multinucleated osteoclasts (Figure 2B, Negative control). Collectively, the findings demonstrated that compound **1** inhibits osteoclast differentiation in a concentration-dependent manner independent of the concurrent proliferation of co-existing preosteoblasts.
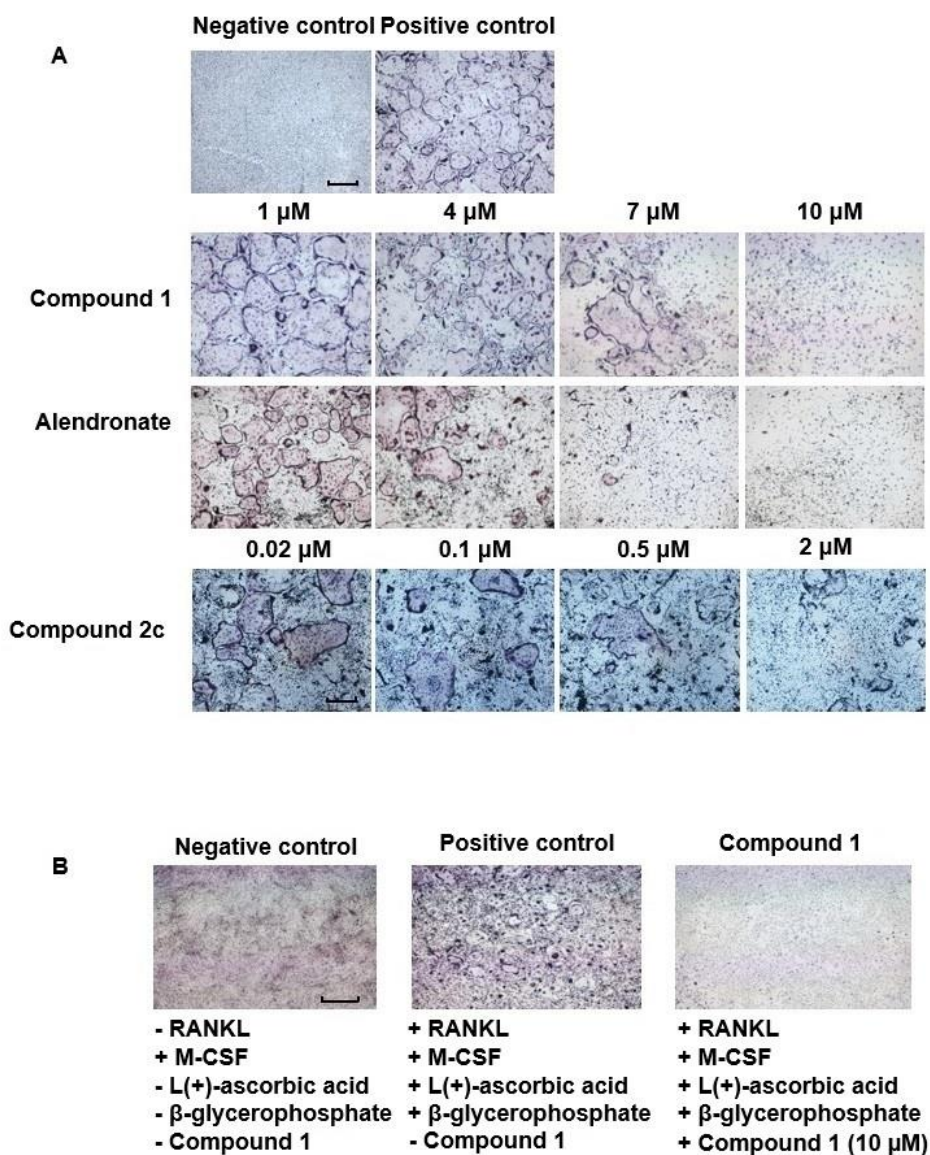
Figure 2. Benzylideneacetone derivatives inhibit RANKL-induced osteoclastogenesis independent of the proliferation of co-existing osteoblast. (A) Comparison of IC_{50} to inhibit osteoclastogenesis between compounds **1** and **2c**, and alendronate. C57BL/6 murine BMM was grown in the presence of M-CSF and RANKL, and a range of concentrations of compound **1** and alendronate (0-10 µM), and compound **2c** (0.02-2 µM). On the sixth day, mature multinucleated osteoclasts were identified by TRAP staining, and observed by an inverted microscope (Magnification: 40 ×. Scale bar = 50 µm). (B) Compound **1** inhibits osteoclast

differentiation while osteoblasts proliferate in the co-culture of preosteoclast and preosteoblast. C57BL6 murine BMM and MC3T3-E1 murine osteoblastic cells were co-cultured in the presence of osteoclast and osteoblast differentiation factors (Positive control). Negative control co-culture was grown in the presence of M-CSF only as a differentiation factor. To test the effects of compound **1** on the proliferation and differentiation of osteoclast and osteoblast, compound **1** was added at a final concentration of 10 µM (Compound **1**). Cells were subject to TRAP staining on the sixth day, and observed by an inverted microscope (Magnification: 40 ×. Scale bar = 50 µm).

Specific SAR of Benzylideneacetone Derivatives Inhibiting Osteoclastogenesis. We next compared different synthetic and natural derivatives of benzylideneacetone in order to elucidate the critical structural determinants necessary for inhibition of osteoclastogenesis (Table 1). Compound **2c** replaced a hydroxyl group with a methoxy group at carbon 4 of catechol of compound **1**, and showed increased osteoclast-inhibitory activity of approximately 70-fold compared to compound **1**, with IC_{50} of approximately 0.11 µM, while sustaining an osteoblast-stimulatory activity as judged by ALP activation. Intriguingly, the replacement of a hydroxyl group by a methoxy group at carbon 3 of catechol of compound **1**, as exemplified by compound **2g**, did not change the osteoclast-inhibitory activity of compound **1** significantly. Similarly, the replacement of a hydroxyl group by a methyl group at carbon 4, or by fluorine (F) at carbon 3 of catechol of compound **1**, exemplified by (*E*)-4-(3-hydroxy-4-methylphenyl)but-3-en-2-one (**2a**) and (*E*)-4-(3-fluoro-4-hydroxyphenyl)-3-buten-2-one (**2h**), did not affect the osteoclast-inhibitory activity of compound **1** significantly. By contrast, the introduction of F or bulky chemical groups at carbon 4 of catechol of compound **1**, exemplified by (*E*)-4-(4-fluoro-3-hydroxyphenyl)but-3-en-2-one (**2b**), (*E*)-4-(3-hydroxy-4-

isopropoxyphenyl)but-3-en-2-one (**2d**), (*E*)-4-(4-benzyloxy-3-hydroxyphenyl)but-3-en-2-one

(**2e**), and (*E*)-4-(4-allyloxy-3-hydroxyphenyl)but-3-en-2-one (**2f**) decreased the activity by 2-3

folds. The findings indicated that the nature of chemical group bound to carbon 4 of catechol

of compound **1**, e.g. hydroxyl, methyl, methoxy, F or bulky chemical groups, determined the

potency to inhibit osteoclastogenesis, suggesting the presence of a specific receptor for a few

benzylideneacetone derivatives on the signaling pathway of osteoclastogenesis. Further, the

removal of a hydroxyl group at carbon 3 of catechol of compound **1** such as (*E*)-4-

hydroxybenzalacetone, decreased the osteoclast-inhibitory activity 4 folds. Notably, the

absence of both hydroxyl groups at carbons 3 and 4 of catechol, as exemplified by *trans*-

cinnamic acid and phenylacetic acid, resulted in a complete loss of osteoclast-inhibitory

activity. Meanwhile, natural products (caffeic acid, chlorogenic acid, neochlorogenic acid)

containing additional functional groups (e.g. carboxylic acid, glycosylate ester) on the aliphatic

ketone substructure of compound **1** showed 5- to 11-fold weaker inhibition of

osteoclastogenesis than that of compound **1**. Likewise, synthetic carboxamides (**3a**, **3b**)

displayed 2- to 3-fold lower osteoclast-inhibitory potency compared with compound **1**.

Similarly, other natural products bearing catechol with a modified aliphatic ketone substructure

of compound **1**, e.g. protocatechualdehyde (**6**), protocatechuic acid, protocatechuic acid methyl

ester, homoprotocatechuic acid, and homoprotocatechuic acid methyl ester, showed

remarkably diminished osteoclast-inhibitory activities. Collectively, the osteoclast-inhibitory

activity of the benzylideneacetone derivatives displayed a highly specific SAR with regard to

the functional group on catechol as well as the aliphatic ketone substructures. Specifically, the

nature of chemical groups bound to carbon 4 of catechol were identified as the key structural

determinants of benzylideneacetone derivatives necessary for inhibition of osteoclastogenesis.

Additionally, the aliphatic ketone substructure was required as an intact side chain for the full

manifestation of the osteoclast-inhibitory activity.

Table 1. Osteoclast Inhibition and Osteoblast Activation by Compound 1 Derivatives

Compounds	TRAP IC_{50} (µM)	% Activation of ALP activity[1]	
		10 µM	50 µM
Osmundacetone (**1**)	7.8 ± 2	120 ± 9	280 ± 60*
2a	5.9 ± 1	100 ± 20	130 ± 30
2b	15 ± 1	100 ± 20	100 ± 20
2c	0.11 ± 0.02	100 ± 20	180 ± 20*
2d	24 ± 3	100 ± 20	94 ± 10
2e	19 ± 5	130 ± 8	140 ± 2
2f	18 ± 8	120 ± 8	140 ± 2
2g	7.5 ± 0.5	110 ± 30	600 ± 70**
2h	8.3 ± 2	100 ± 10	100 ± 20
3a	15 ± 5	110 ± 20	120 ± 40
3b	25 ± 2	110 ± 10	120 ± 20
Protocatechualdehyde (**6**)	15 ± 3	110 ± 10	140 ± 20
(*E*)-4-Hydroxybenzalacetone	32 ± 4	110 ± 8	150 ± 30
Caffeic acid	41 ± 7	120 ± 30	130 ± 40
Neochlorogenic acid	48 ± 4	120 ± 10	170 ± 30*
Chlorogenic acid	86 ± 10	110 ± 4	150 ± 30
Protocatechuic acid	89 ± 10	100 ± 6	140 ± 20
Protocatechuic acid methyl ester	78 ± 10	110 ± 20	100 ± 20
Homoprotocatechuic acid	75 ± 20	120 ± 20	170 ± 20*
Homoprotocatechuic acid methyl ester	80 ± 20	100 ± 20	130 ± 30
trans-Cinnamic acid	>100-	100 ± 30	110 ± 10
Phenylacetic acid	>100	120 ± 30	110 ± 10
Alendronate	3.7 ± 1		
PTH-related peptide (1 µM)		140±20	

[1]% Activation of ALP activity was tested using MC3T3-E1 murine osteoblastic cells.

The values are the mean ± standard deviation (SD) of three independent experiments. [*]

P<0.05. [**] P<0.01

Compound 1 Upregulates the Production of ALP and OCN by Preosteoblasts in a Concentration-Dependent Manner. To assess the osteogenic capability of compound **1**, we tested whether it could induce the production of ALP by preosteoblasts. ALP production in osteoblast-like MC3T3-E1 cells was increased by 280% by compound **1** at a concentration of 50 µM 14 d after administration when compared to control cells (P<0.05) (Table 1), a result consistent with a previous report.[28] Compound **1** increased ALP production by preosteoblasts regardless of its simultaneous inhibition of differentiation of co-existing preosteoclasts (murine BMM). Preosteoblasts and preosteoclasts were co-cultured in the presence of compound **1** (10 µM) as well as differentiation factors for both, which resulted in complete inhibition of osteoclast differentiation on day 6 (Figure 2B, Compound **1**). The co-culture of both cell types continued to grow for 21 d. The activation of ALP production by 10 µM compound **1**-treated preosteoblasts at 7, 14, and 21 d after induction of co-culture differentiation, was 100%, 110%, and 100%, respectively compared with untreated cells, therefore, quite similar to the 120±9% activation of ALP production that occurred 14 d after induction by 10 µM compound **1**-treated osteoblasts grown in the absence of osteoclasts. Overall, the findings indicated that compound **1** activated osteoblastogenesis, while inhibiting osteoclastogenesis.

OCN is expressed only near or at the time of mineralization, i.e., 14-21 d after the induction of osteoblastogenesis.[21] To investigate the effect of compound **1** on the production of OCN by osteoblasts, MC3T3-E1 preosteoblastic cells were cultured in the presence of 50 µM compound **1**. Western blot analysis revealed that OCN production 7, 14, and 21 d after the induction of osteoblastogenesis, increased by 1.8-, 4.1- (P<0.01), and 2.0- (P<0.05) fold, respectively,

compared with untreated positive control cells (Figure 3A,B). In the preosteoblast and preosteoclast co-cultures, supplemented with both osteoblast and osteoclast differentiation factors, compound **1** maintained the capacity to induce production of OCN by osteoblasts, while inhibiting osteoclast differentiation (Figure 3C,D). When preosteoblasts in co-cultures were treated with compound **1** (10 µM), OCN production was similar to that seen with untreated positive control cells. In sum, compound **1** proved capable of increasing the production of ALP and OCN by osteoblasts, while inhibiting osteoclast differentiation.
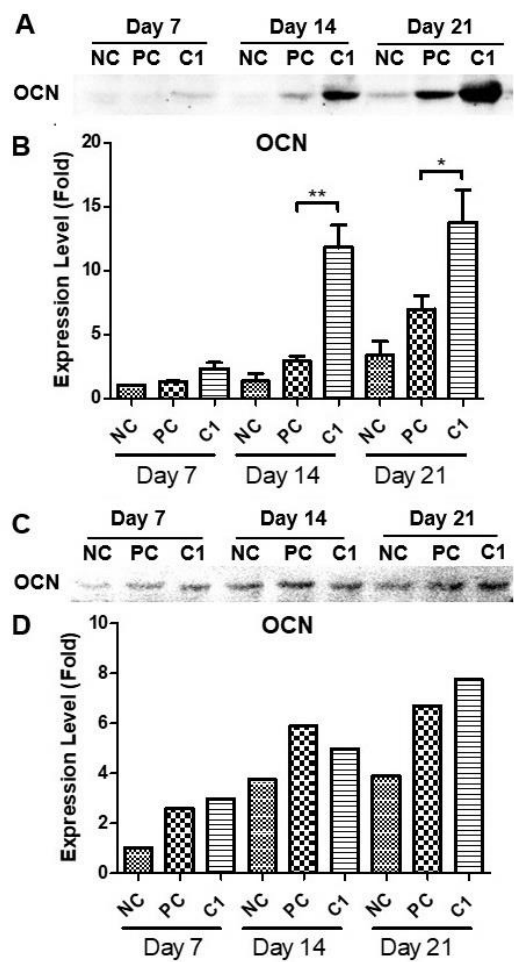

Figure 3. Compound **1** increases the production of OCN during osteoblastogenesis while inhibiting osteoclastogenesis. (A) Compound **1** upregulates the production of OCN by osteoblasts during differentiation. MC3T3-E1 murine osteoblastic cells were induced to

differentiate for 21 d in the presence or absence of compound **1** as described in Experimental

Section. The amounts of OCN in culture media were quantitated by Western blot 7, 14, and 21

d after the induction. **NC** (negative control), cells grown in the absence of osteoblast

differentiation factors; **PC** (positive control), cells grown in the presence of osteoblast

differentiation factors; **C1**, positive control cells grown in the presence of 50 µM compound **1**.

(B) Bar graph representation of mean ± SD of three independent experiments performed as in

(A). *P<0.05, **P<0.01. (C) Compound **1** upregulates the production of OCN by osteoblasts

over the course of differentiation independent of the inhibition of differentiation of co-existing

osteoclasts. MC3T3-E1 murine osteoblastic cells and C57BL6 murine BMM were induced to

differentiate for 21 d in the presence or absence of compound **1** as described in Experimental

Section. The amounts of OCN in culture media were quantitated by Western blot 7, 14, and 21

d after the induction. **NC** (negative control), cells grown in the presence of M-CSF only as a

differentiation factor; **PC** (positive control), cells grown in the presence of osteoblast and

osteoclast differentiation factors; **C1**, positive control cells grown in the presence of 10 µM

compound **1**. (D) Bar graph representation of the levels of OCN in (C).

Specific SAR of Benzylideneacetone Derivatives Activating Osteoblastogenesis.
Chemical modifications of the catechol substructure of compound **1** dramatically altered its

ability to activate ALP production by osteoblasts (Table 1). Compound **2g** which had a

hydroxyl group replaced by a methoxy group at carbon 3 of catechol of compound **1**, displayed

a 2-fold increased capacity to activate osteoblasts to produce ALP at 50 µM, compared with

compound **1** (P<0.01), while showing similar osteoclast-inhibitory potency to that of

compound **1**. By contrast, compound **2c** with a methoxy instead of a hydroxyl at carbon 4 of

catechol resulted in diminished capacity at ALP induction by osteoblasts. Compounds **2d, 2e,**

and **2f** substituting bulky isopropoxy, benzyloxy or allyloxy groups at carbon 4 of catechol, to examine the effect of steric hindrance of functional groups on the stimulation of osteoblastogenesis, displayed remarkably reduced capacities in activating ALP production. Introducing F at carbons 3 or 4 of catechol like in compounds **2b** and **2h**, completely annihilated the capacity of compound **1** to activate ALP production, in contrast with their sustenance of osteoclast-inhibitory potentials. The findings indicated that the nature of chemical group bound to carbon 3 or 4 of catechol of compound **1**, e.g. hydroxyl, methyl, methoxy, F or bulky chemical groups, increased or decreased the potency to activate osteoblastogenesis markedly, suggesting the presence of a specific receptor for a few benzylideneacetone derivatives on the signaling pathway of osteoblastogenesis. Similarly, removal of the hydroxyl at carbon 3 of catechol, e.g. (*E*)-4-hydroxybenzalacetone, also resulted in loss of functionality. Notably, the absence of hydroxyl groups at both carbons 3 and 4 of catechol, exemplified by *trans*-cinnamic acid and phenylacetic acid, resulted in complete loss of ALP-stimulating ability, likewise to their inability to inhibit osteoclast differentiation. Meanwhile, any structural modification of the aliphatic ketone substructure of benzylideneacetone derivatives, i.e., natural products (caffeic acid, chlorogenic acid, neochlorogenic acid) containing additional chemical groups (e.g. carboxylic acid, glycosylate ester), as well as other natural products bearing catechol with a modified aliphatic ketone substructure, e.g. protocatechualdehyde (**6**), protocatechuic acid, protocatechuic acid methyl ester, homoprotocatechuic acid, homoprotocatechuic acid methyl ester, and synthetic carboxamides (**3a**, **3b**) caused remarkable reductions in the capacity to activate ALP production by osteoblast. Collectively, the capacity of benzylideneacetone derivatives to stimulate ALP production by osteoblasts displayed a specific SAR, with any change in the molecular structure remarkably altering the biological activity. Most importantly, the nature of chemical group bound to carbons 3 and 4 of catechol was identified as the key structural determinant.

Benzylideneacetone derivatives also required the intact aliphatic ketone substructure for the full manifestation of its biological potency.

Effects of Compounds 1, 2c, and 2g on the Expression of NF-kB and NFATc1. We investigated the effects of compounds **1**, **2c**, and **2g** on the expression of key transcription factors involved in RANKL-induced osteoclastogenesis, NF-kB[13] and NFATc1[14] (Figure 4A,B). NF-kB expression began to increase in preosteoclasts induced by M-CSF and RANKL (positive control, PC) 2 d after induction of osteoclastogenesis, and then returned to a basal level 5 d after induction (Figure 4A, PC). The preosteoclasts differentiated into mature multinucleated osteoclasts after 6 d. Compound **1** (10 µM) did not affect the NF-kB expression profile of positive control preosteoclasts over the course of osteoclastogenesis significantly (Figure 4A, PC + C**1**), while markedly inhibiting osteoclastogenesis. Intriguingly, the replacement of a hydroxyl group at carbon 4 or 3 of catechol of compound **1** by a methoxy group, compounds **2c** (0.5 µM) and **2g** (10 µM), increased the NF-kB expression of positive control preosteoclasts markedly 1 d after induction and continued to increase the expression during the period of osteoclastogenesis (Figure 4A, PC + **2c**, PC + **2g**), while simultaneously inhibiting osteoclastogenesis. NFATc1 expression increased in positive control preosteoclasts 3 d after RANKL-induced differentiation, and continued to increase (Figure 4B, PC). Compound **1** (10 µM) showed no influence on the NFATc1 expression profile (Figure 4B, PC + C**1**), while inhibiting osteoclastogenesis. Intriguingly, compounds **2c** (0.5 µM) and **2g** (10 µM) reduced the induction of NFATc1 expression over the course of RANKL-induced osteoclastogenesis compared with positive control cells and compound **1**-treated positive control cells. Thus, compounds **2c** and **2g** regulated the expression of NFATc1 as well as NF-kB in a similar way, but differently from compound **1** during RANKL-induced osteoclastogenesis.

Next, we investigated the effects of compounds **1**, **2c**, and **2g** on the expression of NF-kB

and NFATc1 in proliferating murine BMM induced by M-CSF in the absence of RANKL

(negative control, NC). NF-kB expression started to increase remarkably 2 d after

administration of M-CSF (Figure 4A, NC), and the expression profile was not significantly

affected by the presence of compounds **1**, **2g**, and **2c** (Figure 4A, NC + **1**, NC + **2c**, NC + **2g**).

NFATc1 expression in M-CSF-induced murine BMM increased progressively from day 2 to

day 5 (Figure 4B, NC). By contrast, in the presence of compounds **1**, **2g**, and **2c**, the NFATc1

expression induced by M-CSF was remarkably suppressed (Figure 4B, NC + **1**, NC + **2c**, NC

+ **2g**). In sum, compound **1** had no effect on the expression of NF-kB and NFATc1 over the

course of RANKL-induced osteoclastogenesis, while still inhibiting osteoclastogenesis.

Whereas, compounds **2c** and **2g** increased the NF-kB expression remarkably, and diminished

the induction of NFATc1 expression during RANKL-induced osteoclastogenesis, particularly

compound **2c** accompanying a tremendously increased potency inhibiting osteoclastogenesis.

Meanwhile, in M-CSF-induced proliferating BMM in the absence of RANKL, compounds **1**,

2c, and **2g** all suppressed the induction of NFATc1 expression, while not affecting NF-kB
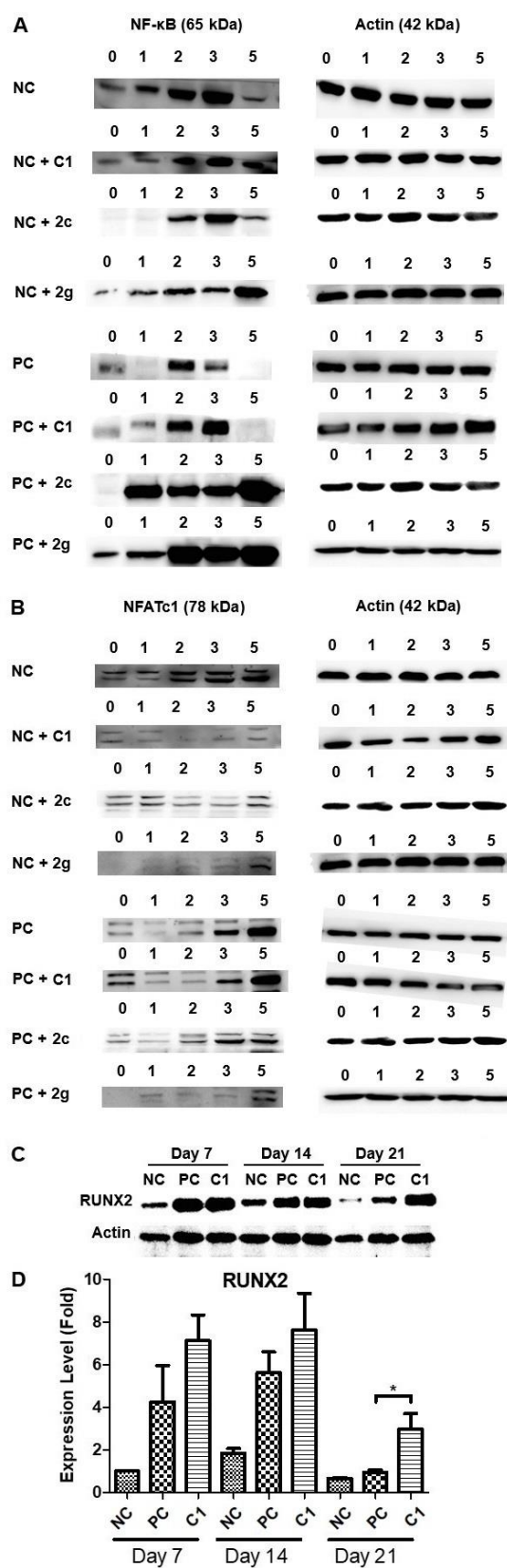
expression significantly.

Figure 4. The effects of benzylideneacetone derivatives on the expression of osteoclast transcription factors, NF-kB and NFATc1, and an osteoblast transcription factor, RUNX2 over the course of osteoclastogenesis and osteoblastogenesis. (A) Compound **1** did not affect NF-kB expression, but compound **2c** and **2g** increased NF-kB expression markedly over the course of RANKL-induced osteoclastogenesis, while, during M-CSF-induced BMM proliferation, all of compounds **1**, **2c**, and **2g** did not affect NF-kB expression significantly. C57BL/6 murine BMM were induced to differentiate, and harvested 0, 1, 2, 3, and 5 d after the induction. NF-kB expression was quantitated by Western blot. **NC** (negative control): BMM grown in the presence of M-CSF alone as a differentiation factor. **NC + C1**: negative control BMM treated with 10 µM compound **1**. **NC + 2c**: negative control BMM treated with 0.5 µM compound **2c**. **NC + 2g**: negative control BMM treated with 10 µM compound **2c. PC** (positive control): BMM grown in the presence of M-CSF and RANKL. **PC + C1**: positive control BMM treated with 10 µM compound **1**. **PC + 2c**: positive control BMM treated with 0.5 µM compound **2c**. **PC + 2g**: positive control BMM treated with 10 µM compound **2g.** (B) Compound **1** did not affect NFATc1 expression, but compound **2c** and **2g** suppressed the induction of NFATc1 expression markedly over the course of RANKL-induced osteoclastogenesis, while, during M-CSF-induced BMM proliferation, all of compounds **1**, **2c**, and **2g** suppressed NFATc1 expression. The murine BMM over the course of osteoclastogenesis was prepared as in (A). NFATc1 expression was quantitated by Western blot. **NC**, **NC + C1**, **NC + 2c**, **NC + 2g**, **PC**, **PC + C1**, **PC + 2c** and **PC + 2g** designate the same as in (A). (C) Compound **1** increased the expression of RUNX2 in osteoblasts during differentiation. MC3T3-E1 murine osteoblastic cells were induced to differentiate in the presence or absence of 50 µM compound **1** for 21 d. The cells were harvested 7, 14, and 21 d after the induction. RUNX2 expression was quantitated by Western blot. **NC** (negative control), cells grown in the absence of osteoblast differentiation factors; **PC** (positive control), cells grown in the presence of osteoblast differentiation factors;

C1, positive control cells grown in the presence of compound **1**. (D) Bar graph representation of mean ± SD of three independent experiments performed as described in (C). *P<0.05.

Compound 1 Upregulates the Expression of RUNX2 during Osteoblastogenesis. Next, we tested if compound **1** increased the expression of RUNX2, a transcription factor and an early differentiation marker that increases bone formation by stimulating the transcription of ALP and OCN in preosteoblasts.[19] Compound **1** increased the expression of RUNX2 in preosteoblasts over the course of differentiation by 1.7, 1.4, and 3.2 (P<0.05) folds 7, 14, and 21 d after induction, respectively, compared with the corresponding compound **1**-untreated positive control cells (Figure. 4C,D, PC, C**1**). This finding indicated that compound **1** upregulated and prolonged the induction of RUNX2 expression in preosteoblasts, partly explaining the molecular mechanism behind the ability of compound **1** to activate osteoblastogenesis.

Pharmacokinetic Behavior of Compounds 1 and 2c. Next, we investigated the pharmacokinetic (PK) behavior of compounds **1** and **2c** (Table 2). Plasma concentration vs time plots for compounds **1** and **2c** were obtained to extract important PK parameters (Supporting Information 3). The plasma concentrations represented the sum of unbound compounds free from plasma proteins and those reversibly bound to plasma proteins, based on the experimental procedure to measure the concentrations. $T_{1/2}$ (terminal half-life) is the time required to reach half the plasma concentration at pseudo-equilibrium, a parameter controlled by the volume of distribution and plasma clearance mainly dependent on hepatic clearance (metabolic stability and biliary clearance) and renal clearance, when absorption is not an influencing factor, e.g. intravenous (IV) administration.[34] $T_{1/2}$ of IV-administered compounds **1** and **2c** were in proportion to AUC_{∞} (area under the plasma concentration-time curve from

time zero to infinity, indicating total blood exposure concentration). AUC_∞ of compounds **1** and **2c** administered IV at 2 mg/kg were 39 and 100 nM·h, respectively, and $T_{1/2}$ of those were 0.40 and 1.0 h, respectively, indicating that compound **2c** is more stable than compound **1** in blood plasma. The difference between AUC_∞ of compounds **1** and **2c** might be ascribed to the different efficiency of plasma clearance system for each compound. On *per os* (PO) administration, the rate and extent of absorption is more reflected in $T_{1/2}$ than the elimination process in plasma.[34] $T_{1/2}$ of compound **1** administered PO at 10 and 50 mg/kg (2.1 and 3.1 h, respectively) was much higher than $T_{1/2}$ of the IV administration at 2 mg/kg (0.40 h). The finding might be due to much higher AUC_∞ of compound **1** administered PO at 10 and 50 mg/kg (140 and 660 nM·h, respectively) than AUC_∞ of compound **1** administered IV at 2 mg/kg (39 nM·h). The high value of AUC_∞ of PO-administered compound **1** might be ascribed to the high bioavailability (F) of compound **1** (66 and 76% at 10 and 50 mg/kg), indicating $AUC_{P.O.}/AUC_{I.V.}$. F of compound **1** was 2-3 fold higher than 26-29% of compound **2c** in the dose range of 10-50 mg/kg PO. As might be deduced based on $T_{1/2}$ on IV administration and F, AUC_∞ of compounds **1** and **2c** administered PO at 10 or 50 mg/kg were similar in systemic circulation, 140 or 660 nM·h for compound **1**, and 140 or 720 nM·h for compound **2c**, respectively. Likewise, C_{max} (maximum plasma concentration) of compounds **1** and **2c** administered PO were not different significantly. C_{max} of compound **2c** administered PO at 10 and 50 mg/kg was 0.16 and 0.88 μM, respectively, which were higher than IC_{50} of the compound (0.11 μM) to inhibit osteoclastogenesis. The pharmacokinetic behavior of compound **1** via oral administration belongs to two-compartment model, which divides the body into central and peripheral compartment. The central compartment consists of the plasma where the distribution of the compound **1** is practically instantaneous (distribution phase). The peripheral compartment consists of tissues where the distribution of compounds is slower. The decrease of compound **1** in peripheral compartment is likely attributed to drug metabolism and

excretion (elimination phase). So we calculated $T_{1/2}$ of orally administered compound **1** in elimination phase. However, the pharmacokinetic behavior of compound **1** via IV route showed single compartment model where the concentration of compound **1** rapidly decreased and disappeared in plasma.

Table 2. Pharmacokinetic Parameters of Compounds 1 and 2c

Compounds	Route	Dose (mg/kg)	$T_{1/2}$ (h)	C_{max} (nM)	AUC_{∞} (nM·h)	F (%)
1	IV	2	0.40	-	39 ± 10	-
	PO	10	2.1	200 ± 60	140 ± 10	66
	PO	50	3.1	1100 ± 300	660 ± 200	76
2c	IV	2	1.0	-	100 ± 5	-
	PO	10	1.2	160 ± 50	140 ± 30	26
	PO	50	2.2	880 ± 300	720 ± 400	29

$T_{1/2}$; terminal half-life. C_{max}; maximum plasma concentration. AUC_{∞}; area under the plasma concentration-time curve from time zero to infinity, indicating total blood exposure concentration. F; bioavailability indicating $AUC_{P.O.}/AUC_{I.V.} \times 100$. The values of C_{max} and AUC_{∞} are the mean ± SD obtained from three male ICR mice.

Preventive Effects of Compounds 1, 2c and 2g on OVX-Induced Osteoporosis. The potential of benzylideneacetone derivatives as novel anti-osteoporotic agents was tested in OVX-induced osteoporotic ddY mice. Compound **1** (10 mg/kg/d), compound **2g** (10 mg/kg/d) or compound **2c** (1 and 10 mg/kg/d) in 300 µL PBS were administered PO to OVX mice for 4 weeks using gavage, beginning 1 week after OVX. Alendronate (10 mg/kg/d) in 300 µL PBS was administered PO to OVX mice as a reference compound. PBS as a vehicle was administered 300 µL/d PO to OVX and sham controls. Body weights of OVX control, benzylideneacetone derivatives- or alendronate-administered OVX mice increased remarkably 5 weeks after OVX compared with sham control (Supporting Information 4). Femur and tibia

of each mouse were subjected to scanning (SkyScan1173 Ver. 1.6, Bruker-CT, Kontich, Belgium), and were reconstructed using Nrecon Ver. 1.7.0.4 (Bruker, Kontich, Belgium) based on the Feldkamp algorithm. Representative images of CT scans and 3-D representations of each group are presented in Figure 5, and those of all mice in all experimental groups are presented in Supporting Information 5. After reconstruction of the femur images of all mice in each group, the histomorphometrical indices and regenerated bone volume, including bone mineral density (BMD, g/mm^3), percent bone volume (BV/TV, %), crossectional thickness (Cs.Th, mm), trabecular number (Tb.N, number/mm), trabecular thickness (Tb.Th, mm), trabecular separation (Tb.Sp, mm), and new bone volume (NBV, mm^3) were obtained (Figure 6, Supporting Information 6). OVX mice showed significantly deteriorated histomorphometric indices of bone including BMD, BV/TV, Cs.Th, Tb.N, Tb.Th, Tb.Sp, and NBV, displaying osteoporotic features compared with sham control. Oral administration of benzylideneacetone derivatives or alendronate for 28 d to OVX mice led to the recovery of all the histomorphometric indices mainly in proportion to their potencies at inhibiting osteoclastogenesis. The BMD of femur increased significantly ($P<0.01$) in all benzylideneacetone derivatives- and alendronate-treated groups with the highest seen with compound **2c** (1 or 10 mg/kg/d) ($P<0.001$) and alendronate (10 mg/kg/d) ($P<0.01$) groups compared with OVX control. BV/TV was recovered significantly ($P<0.05$) in all benzlideneacetone derivatives- and alendronate-treated groups with the highest seen in compound **2c** (1 or 10 mg/kg/d) ($P<0.001$) and alendronate (10 mg/kg/d) ($P<0.05$) groups compared with OVX control. Cs.Th was significantly recovered ($P<0.05$) in compound **2c** (1 mg/kg/d) and alendronate (10 mg/kg/d) groups up to the levels comparable with sham control, and compounds **1**, **2c** and **2g** (10 mg/kg/d, respectively) groups also showed recoveries in Cs.Th compared with OVX control. Tb.N increased significantly in compound **2c** (1 mg/kg/d) ($P<0.01$), compound **2c** (10 mg/kg/d) ($P<0.05$) and alendronate (10 mg/kg/d) ($P<0.05$) groups,

and compounds **1** and **2g** (10 mg/kg/d, respectively) groups also showed increases compared with OVX control. Tb.Th was significantly recovered in compound **2c** (10 mg/kg/d) group (P<0.01), and compound **2c** (1 mg/kg/d), compound **1** (10 mg/kg/d), and compound **2g** (10 mg/kg/d) groups also showed recoveries compared with OVX control. By contrast, alendronate (10 mg/kg/d) failed to increase Tb.Th compared with OVX control. Tb.Sp was significantly reduced (P<0.05) by compound **2c** (1 mg/kg/d) and alendronate (10 mg/kg/d) compared with OVX control, up to the levels comparable with the sham control, and Tb.Sp of compounds **1**, **2c** and **2g** (10 mg/kg/d, respectively) groups also decreased compared with OVX control. NBV increased significantly (P<0.05) with compound **2c** (1 or 10 mg/kg/d) compared with OVX control, and NBV of compounds **1, 2g**, and alendronate (10 mg/kg/d, respectively) groups also increased compared with OVX control.

Collectively, the findings demonstrated that all benzylideneacetone derivatives display the capacity to prevent bone loss presumably through their capacity to inhibit osteoclastogenesis. C_{max} of 0.16 μM for compound **2c** administered 10 mg/kg PO was higher than IC_{50} inhibiting osteoclastogenesis *in vitro*, explaining its osteoporosis-preventive efficacy. The *in vivo* osteoporosis-preventive effect of 1 mg/kg/d compound **2c** implied that the effective therapeutic concentration of compound **2c** was reached *in vivo* by the administration of 1 mg/kg/d PO to show the efficacy comparable to alendronate administration of 10-fold more daily dose, which was ascribed to 30-fold stronger potential of compound **2c** for *in vitro* osteoclast inhibition than that of alendronate. While C_{max} of 0.20 μM for compound **1** administered 10 mg/kg/d PO was lower than its *in vitro* IC_{50} of 7.8 μM against osteoclastogenesis, compounds **1** and **2g** (IC_{50} 7.5 μM) exhibited an *in vivo* osteoporosis-preventive effect up to half the level of improvement by alendronate (IC_{50} 3.7 μM), which indicated that the *in vitro* osteoclastogenesis-inhibitory potencies were reflected proportionally in the degree of *in vivo* osteoporosis-preventive efficacy. Even though C_{max} of 0.20 μM for compound **1** was much lower than the concentration

substantially inducing osteoblastogenesis *in vitro*, it was suggested that the osteoblastogenesis-stimulatory potential of compound **1** may be sustained to preserve normal osteoblastic activity *in vivo* while inhibiting osteoclast, based on the fact that compound **1** caused higher Tb.Th than alendronate despite its IC_{50} of half the level of alendronate inhibiting osteoclastogenesis.
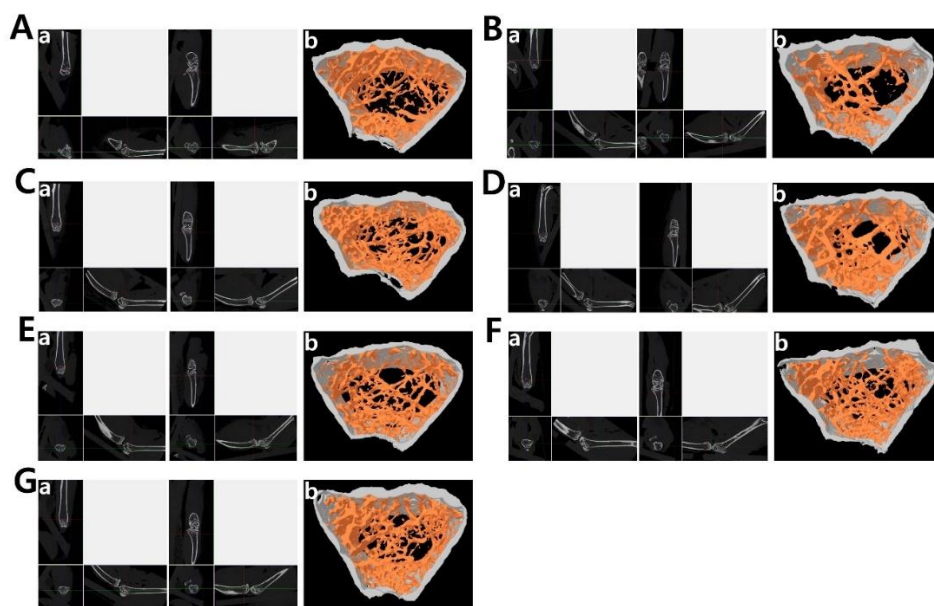

Figure 5. Representative CT and 3-D images of femur and tibia of mice in different experimental groups. Beginning a week after OVX surgery, mice received 10 mg/kg/d of compounds **1**, **2g**, or alendronate, or 1 or 10 mg/kg/d of compound **2c** in 300 µL of 0.5% (v/v) DMSO-containing PBS PO once daily using gavage. Sham and OVX control received 300 µL of 0.5% (v/v) DMSO-containing PBS once daily. After 28 d. mice were euthanized, and femur and tibia of each mouse were fixed and subject to CT analysis to obtain CT and 3-D images. The results of anti-osteoporotic effects of the benzylideneacetone derivatives were compared with those of alendronate. A. Sham control. B. OVX control. C. Alendronate 10 mg/kg/d. D. Compound **1** 10 mg/kg/d. E. Compound **2g** 10 mg/kg/d. F. Compound **2c** 10 mg/kg/d. G.

Compound **2c** 1 mg/kg/d. a. CT images of a region of interest, b. 3-D images of a region of
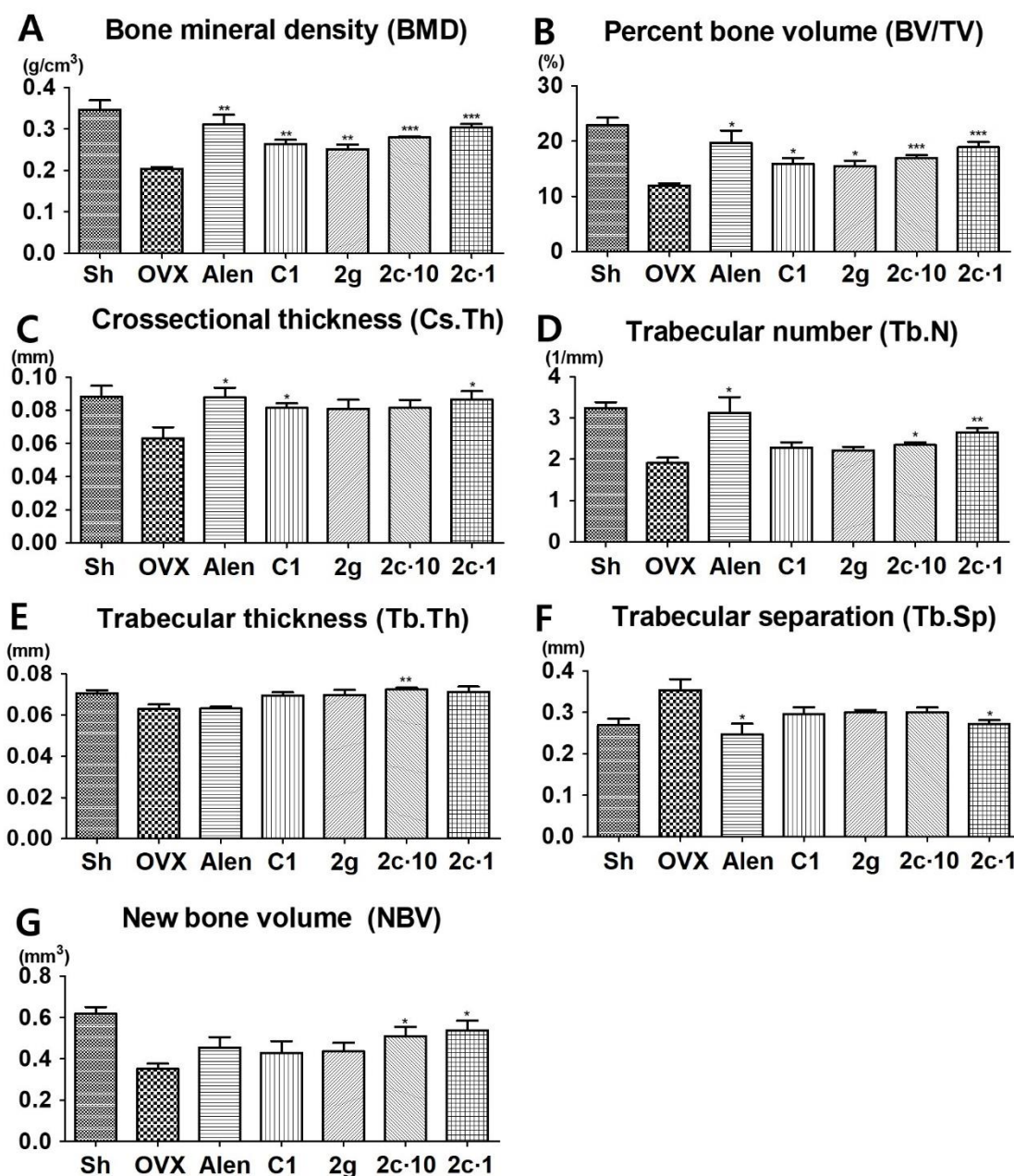
interest. OVX = ovariectomy.

Figure 6. Histomorphometrical indices and regenerated bone volume after reconstruction of

the CT images of femur of each mouse in different experimental groups. The CT images of

femur of each mouse in all groups were reconstructed using a computer program, Nrecon Ver.

1.7.0.4 based on the Feldkamp algorithm to determine histomorphometrical indices in defect areas. The reconstruction by NRecon was performed using the same applied scan and reconstruction parameters for all specimens. NBV (new bone volume) was calculated within the regions of interest. BMD (bone mineral density, g/mm^3), BV/TV (percent bone volume, %), Cs.Th (crossectional thickness, mm), Tb.N (trabecular number, number/mm), Tb.Th (trabecular thickness, mm), Tb.Sp (trabecular separation, mm), NBV (mm^3). Compounds **1**, **2c** and **2g** = test compounds. Alendronate = a reference compound. **Sh** = sham control mice. **OVX** = ovariectomy control mice. **Alen** = alendronate 10 mg/kg/d. **C1** = compound **1** 10 mg/kg/d. **2g** = compound **2g** 10 mg/kg/d. **2c·10** = compound **2c** 10 mg/kg/d. **2c·1** = compound **2c** 1 mg/kg/d. Values are expressed as mean ± SD of four mice. *P<0.05, **P<0.01, ***P<0.001.

Cancer-Specific Cytotoxicity of Benzylideneacetone Derivatives. Any compound with LD_{50} less than 100 µM is considered cytotoxic and antiproliferative.[35] Accordingly, compound **1** did not exhibit cytotoxicity against normal cell lines based on 3-(4,5-dimethylthiazol-2-yl)-2,5-diphenyltetrazolium bromide (MTT) assay used to estimate cellular growth and survival (Supporting Information 7).[36] Specifically, compound **1** displayed negligible cytotoxicity against human adipose-derived mesenchymal stem cells, HaCaT human epidermal keratinocytes, and NIH3T3 mouse embryo fibroblasts with LD_{50} values of 2,800, 3500, and >5,000 µM, respectively. It did however, show weak antiproliferative activity on RAW264.7 murine macrophage cell line with LD_{50} of 500 µM in the absence of RANKL, suggesting that compound **1** may suppress the proliferation of a few phagocytic cells at high concentrations. This supports a report showing that compound **1** suppressed the production of immune mediators.[26] It exhibited considerable cytotoxicity against cancer cell lines including AGS human gastric adenocarcinoma, PC3 human prostate adenocarcinoma, and B16F10 mouse

melanoma with LD_{50} values of 60, 66, and 65 µM, respectively, supporting a cancer-specific cytotoxicity that has been reported.[29] Compounds **2c and 2g**, did not exert an antiproliferative activity on preosteoclastic RAW264.7 macrophage cells with LD_{50} of >5,000 µM in the absence of RANKL in spite of a strong potency to inhibit RANKL-induced osteoclastogenesis, suggesting that compound **2c** and **2g** may not have any antiproliferative activity on macrophages that are not undergoing osteoclastogenesis. Compound **2c** displayed a relatively high antiproliferative activity on a few cancer cell lines including T24 human bladder carcinoma cells with LD_{50} of 180 µM, and compound **2g** on HCT116 human colon carcinoma cells with LD_{50} of 310 µM in line with its specific cytotoxicity against HT-29 human colon cancer cells.[33] Overall, compounds **1**, **2c** and **2g** showed negligible anti-proliferative effects against normal cell lines tested, but exhibited significant cytotoxicity against a few cancer cell lines.

DISCUSSION AND CONCLUSIONS

We demonstrated that a few benzylideneacetone derivatives strongly inhibit osteoclastogenesis and activate osteoblastogenesis independently, which stands in contrast to earlier observations that the differentiation of osteoclasts and osteoblasts tends to occur in parallel.[23,24] In particular, it is worth noting that the *in vitro* capacities of a few benzylideneacetone derivatives were reflected in the management of OVX-induced osteoporosis mainly in proportion to their *in vitro* potencies to inhibit osteoclastogenesis. Compound **2c** administered 1 mg/kg/d PO displayed a preventive effect on the development of osteoporosis in OVX mice comparable to that of 10 mg/kg/d alendronate. The observation was consistent with the finding that IC_{50} of compound **2c** to inhibit *in vitro* osteoclastogenesis of C57BL/6 murine BMM was 30-fold stronger than 3.7 µM of alendronate. The IC_{50} value of alendronate in our setting was

compatible with the previous finding that IC_{50} of alendronate was 460 nM against recombinant human farnesyl diphosphate synthase, 1.7 µM against isopentenyl diphosphate isomerase and farnesyl diphosphate synthase in a liver cytosolic extract, and 15 µM at murine osteoclast cellular level to inhibit protein prenylation and mevalonate-derived lipid synthesis.[37] C_{max} of compounds **1** and **2c** administered a single dose of 10 mg/kg PO was 200 and 160 nM, respectively, and thus C_{max} of compound **2c** administered 1 mg/kg/d PO might be much lower than *in vitro* IC_{50} against osteoclastogenesis. However, the finding that 1 mg/kg/d compound **2c** PO exhibited expected pharmacological effects comparable to those of 10 mg/kg/d alendronate may indicate that very low target engagement is required for desired therapeutic effects of compound **2c**. Intriguingly, alendronate displayed osteoclastogenesis-inhibitory effects at *in vivo* C_{max} concentrations much lower than *in vitro* IC_{50} at enzymatic as well as cellular levels. C_{max} of alendronate was 227−260 nM after the single 70 mg dose of three generic and reference products, which was slightly higher than C_{max} of compound **1** and **2c** (200 and 160 nM at single dose of 10 mg/kg PO, respectively).[38] In other study, healthy males were administered single 70 mg dose of alendronate sodium regimens, reference and bioequivalent test drugs, where C_{max} of each was 234 and 199 nM, respectively, which were slightly higher than C_{max} of single dose of 10 mg/kg PO compound **1** and **2c**.[39] Thus, we suggest the possibility that compounds **1** and **2c** may also exert desired therapeutic effects toward the management of osteoporosis at C_{max} concentrations much lower than *in vitro* IC_{50}, and that low target engagement may be required at the molecular level inside cells to block osteoclastogenesis to occur, to similar degrees to alendronate.

SAR analysis conclusively demonstrated that any slight modification in catechol and aliphatic ketone substructures of benzylideneacetone derivatives affect differentially the potencies to inhibit osteoclastogenesis and activate osteoblastogenesis. Indeed, the replacement of a hydroxyl group at carbon 4 of catechol of compound **1** increased IC_{50} against

osteoclastogenesis 70 folds, but decreased the induction of ALP production by osteoblast. The replacement of a hydroxyl group at carbon 3 of catechol of compound **1** increased ALP production by osteoblast 2 folds, but did not affect IC_{50} against osteoclastogenesis. Introducing F at carbon 3 or 4 of catechol of compound **1** like in compounds **2b** and **2h**, did not affect the capacity to inhibit osteoclastogenesis significantly, in contrast with complete loss of the activity to induce ALP production by osteoblasts. SAR of benzylideneacetone derivatives independently regulating osteoclast and osteoblast may indicate the presence of different specific receptors for the compounds in each cell type.

Compound **1** dramatically suppressed osteoclastogenesis without significantly affecting the induction of expression of NF-kB and NFATc1, two key transcription factors participating in RANKL-induced osteoclastogenesis.[13,14] It may be that the action of compound **1** is not strong enough to change the expression profiles of NF-kB and NFATc1 over the course of osteoclastogenesis, but strong enough to chemically modify functional groups on NF-kB and NFATc1, especially phosphorylation of NF-kB, which is important for the regulation of its transcriptional activity. Others have reported that compound **1** blocked IkBalpha kinase activation and NF-kB-regulated gene expression.[40,41] In our study, during M-CSF-stimulated murine BMM proliferation, compound **1** reduced the induction of NFATc1 downstream of NF-κB, whereas the compound did not affect the NFATc1 expression during RANKL-induced osteoclastogenesis (Figure 4B, NC + C**1**, PC + C**1**). The finding suggested that compound **1** may have a target molecule between NF-κB and NFATc1 on M-CSF-induced signaling pathway of BMM that does not exist on RANKL-induced signaling pathway of BMM. Compound **2c** increased NF-kB expression markedly and suppressed the induction of NFATc1 expression over the course of RANKL-induced osteoclastogenesis, accompanying a tremendously increased potency to inhibit osteoclastogenesis. Thus, it appeared that the increased expression of NF-κB led to the suppression of NFATc1 expression during

osteoclastogenesis. The finding is inconsistent with previous findings that RANKL-induced activation of NF-κB induces downstream molecules including NFATc1.[42] Future studies will be necessary to determine the molecular mechanism underlying this finding. Compounds **2c** and **2g** increased the NF-kB expression during RANKL-induced osteoclastogenesis of BMM markedly, but did not affect the NF-kB expression during M-CSF-triggered BMM proliferation significantly (Figure 4A). The finding might indicate that compounds **2c** and **2g** have a molecular target upstream of NF-kB on RANKL-induced osteoclastogenesis signaling pathway that does not exist on M-CSF-induced signaling pathway. Further, compounds **2c** and **2g** likely have the same target molecule, but different affinities toward the molecule. Collectively, it appears that pathways of RANKL-induced osteoclastogenesis of BMM and M-CSF-induced BMM proliferation, share common components, i.e., NF-kB and NFATc1, and also contain different sets of intrinsic components, e.g. those upstream of NF-kB as well as between NF-kB and NFATc1. Compounds **1**, **2c** and **2g** might specifically target these to regulate the inductions of NF-kB and NFATc1 differentially between the two signaling pathways, a conclusion that is compatible with the notion of osteoimmunology that mechanisms are shared between the immune and bone systems that conduct a crosstalk each other.[22]

Compound **1** and its derivatives, may be considered pan assay interference compounds (PAINS) and covalent modifiers based on the fact that it contains substructures including low risk catechol and high risk aliphatic ketones such as high risk Michael acceptors, covalent Michael acceptors, and covalent α,β-unsaturated carbonyl compound, which are prone to covalent bonding rather than reversible specific binding.[43-45] In drug development, biologically active compounds are classified into true hits, potential hits, and false positives. We conclude that compound **1** and its derivatives may be considered true hits that function by reversible specific binding with a cellular target, rather than irreversible nonspecific covalent bonding,

based on the following. First of all, *in vitro* potency of a few benzylideneacetone derivatives in terms of osteoclastogenic inhibition were reflected proportionally in the degree to which they could ameliorate histomorphometrical indices and bone regeneration in an osteoporosis animal model. Next, we disturbed the catechol substructure of benzylideneacetone by substituting hydroxyl groups with other functional groups to verify that the candidate derivatives are likely true hits for new therapeutics, and to reduce the possibility of developing covalent modifiers. As a result, the aliphatic ketone substructure appears unlikely to act as a covalent modifier based on following findings. Without any modification of the aliphatic ketone substructure of compound **1**, replacement of either one of the catechol hydroxyls with a methoxy group resulted in a marked increase in osteoclastogenic inhibition or osteoblastogenic activation. (*E*)-4-Hydroxybenzalacetone that lacks a hydroxyl group at the catechol carbon 3 of compound **1** with the intact aliphatic chain substructure, showed markedly diminished osteoclast-inhibitory and osteoblast-stimulatory activities, compared with compound **1**. *trans*-Cinnamic acid that is devoid of two hydroxyl groups of catechol of compound **1** with the intact α,β-unsaturated carbonyl group completely lost the capacities of osteoclastogenesis inhibition and osteoblastogenesis activation. Thus, it appeared implausible that irreversible nonspecific covalent bonding between the aliphatic ketone substructure and its target in osteoclasts or osteoblasts is a crucial mechanism behind the biological activities. Further, the replacement of any catechol hydroxyl with F without changing the structure of aliphatic ketone chain of compound **1**, exemplified by compounds **2b** and **2h**, completely abolished the osteoblast-stimulatory activity, implying that covalent bond formation between the aliphatic ketone substructure and a target molecule in osteoblast is unlikely a crucial element of compound **1** activating osteoblastogenesis. In sum, these findings support the notion that a few benzylideneacetone derivatives do not function by irreversible nonspecific covalent bond formation between the aliphatic ketone substructure and a target molecule in osteoclast or

osteoblast. Likewise, an irreversible nonspecific covalent bond formation between the catechol substructure of benzylideneacetone derivatives and their targets does not appear to be the key element behind their biological activities. The finding that perturbing the catechol substructure of compound **1** by replacing hydroxyl groups with a methoxy group resulted in greater enhancement of osteoclastogenic inhibition or osteoblastogenic activation rather than their elimination, also implied that a putative covalent bond between catechol and a target in osteoclast or osteoblast is unlikely to be the mechanism to regulate the activity of osteoclast or osteoblast. This hypothesis is further supported by the finding that the replacement of a hydroxyl group at carbon 4 of catechol of compound **1** with methyl or F groups exemplified by compounds **2a** and **2b**, and at carbon 3 with methoxy or F groups exemplified by compounds **2g** and **2h**, did not alter the osteoclastogenesis-inhibitory potency of compound **1** significantly, which would not have occurred if the formation of an irreversible nonspecific covalent bond of catechol with a target molecule in osteoclast was the mode of action. Collectively, it appeared that a few benzylideneacetone derivatives may exert their biological effects by reversibly binding specific cellular targets in osteoclast and osteoblast.

Still, there is the possibility that the benzylideneacetone derivatives could be specific covalent inhibitors, possibly reversible, against their targets, or covalent modifiers that may react with off-target biological nucleophiles forming irreversible adducts. However, some covalent modifiers have been developed into drugs successfully. For example, afatinib and dacomitinib, irreversible ErbB family blockers, could be developed as anticancer agents.[46] Acrylamide-based inhibitors forming reversible covalent bonds with noncatalytic cysteine targets enhanced ligand efficiency with high pharmacological potency and selectivity.[47,48] Also, Michael acceptor containing compounds were demonstrated to be an efficient 5-lipoxygenase inhibitor targeting the surface cysteines.[49] These considerations led us to believe that a few benzylideneacetone derivatives are potential hit compounds for osteopenic diseases.

The biological properties of a few benzylideneacetone derivatives have considerable clinical implications for a variety of bone diseases. Bone maintains a dynamic state in adults, with 15% of trabecular bone and 3% of cortical bone replaced every year in order to adapt to changing mechanical loads and restoration of microdamage during normal use. [1] As part of the normal aging process, both men and women show a reduced number and vigor of osteoblasts, leading to reduced bone formation and slower healing of bone fractures. In the postmenopausal stage, low levels of estrogen lead to increased osteoclastogenesis.[50] The main focus of current efforts to counteract bone loss-related diseases is the suppression of osteoclast differentiation, using inhibitors of osteoclast differentiation, including bisphosphonate drugs and Denosumab, a monoclonal antibody to RANKL.[3,51] Additionally, PTH has a significant role as an anabolic drug for osteoporosis by activating osteoblastogenesis.[4] However, the clinical use of bisphosphonates such as alendronate, ibandronate and zoledronic acid,[52,53] Denosumab,[54] and PTH regimen[55] is accompanied by adverse effects and contraindications, limiting their long-term use for complete recovery. Unfortunately, there are few new drug candidates with greater therapeutic efficacy and fewer adverse effects, on the horizon. Therefore, in this setting, compounds **2c** and **2g** may be promising candidates as novel therapeutics for osteoporosis, given their potent osteoclast-inhibitory activity, osteoblast-stimulatory activity, and lack of apparent cytotoxicity. In particular, compound **2c** displayed 30-fold more potent osteoclastogenic-inhibitory activity than alendronate, which may enable the administration of much lower doses of the compound than is necessary for alendronate, decreasing the risk of adverse effects. Meanwhile, any change in osteoclast differentiation tends to be concomitant with parallel changes in osteoblast differentiation due to intricate coupling mechanisms between osteoclasts and osteoblasts that maintain the coordination between bone formation and resorption.[22] This phenomenon interferes with therapeutic interventions for osteopenic diseases. Thus, a few anabolic approaches focus on uncoupling osteoblast action from osteoclast

formation. In this context, the truly important advantage of compounds **2c** and **2g** in terms of osteoporosis therapeutics includes their dual potential to inhibit osteoclastogenesis and activate osteoblastogenesis independently. Bone attracts cancer cells often with fatal outcomes.[56] Bone marrow cells interact with tumor cells to facilitate successful metastases.[57] Metastasizing tumor cells mobilize osteoclasts to sculpt the bone microenvironment and carve a niche for the promotion of tumor growth and bone invasion.[6] Zoledronic acid is an FDA-approved drug used to prevent and treat cancer metastasis to bone, which targets osteoclasts.[8,58,59] Intriguingly, co-administration of anabolic PTH along with zoledronic acid further reduces prostate cancer bone metastasis.[5] Therefore, the development of an agent with a capacity for both osteoclast inhibition and osteoblast activation may enhance therapeutic effects for cancer bone metastasis. Compounds **2c** and **2g** therefore, may have a therapeutic edge for cancer bone metastasis, and could possibly be reinforced by the anticancer activities we noted (Supplementary Information 7) as well as previous reports.[33,60] Currently, there are no drugs for resolving rheumatoid arthritis aggravated by the autoimmune antibodies that stimulate osteoclastogenesis.[61] Therapeutic agents act by ameliorating symptoms such as pain and edema, or by delaying disease progression. One of the most popular prescriptions involves disease-modifying anti-rheumatic drugs (DMARDs) such as methotrexate in combination with biologics, especially inhibitors of TNF-alpha, a pro-inflammatory cytokine. Although new biologics are being continuously developed, new medications with similar or better therapeutic efficacy are yet to be found. Compound **1** may be therapeutically useful based on its capacity to inhibit osteoclastogenesis as well as previously reported immunomodulatory effects inhibiting the production of immune mediators that mediate the pathophysiology of rheumatoid arthritis.[26,27] Indeed, compound **1** is a component of the rhizome of *Osmunda* genus, and *Osmunda regalis* L. has been used as a highly efficient ethnopharmacology agent for rheumatoid arthritis in Spain. Due to rising demand for this plant, consumption of *Osmunda regalis* L. has evoked

awareness of overexploitation and prompted efforts at conservation in northern Spain.[30] The

possibility that compound **1** may be one of the effective active ingredients that contributes to

therapeutic efficacy of the plant for rheumatoid arthritis has yet to be established.

In conclusion, a search for the mechanism of action by which benzylideneacetone derivatives

inhibit osteoclastogenesis and activate osteoblastogenesis independently, is anticipated to

provide new insights into bone homeostasis with clinical implications for the management of

osteoclast-related bone diseases.

EXPERIMENTAL SECTION

Synthesis of Benzylideneacetone Derivatives. Compounds **2a−h** and **3a, b** were

synthesized chemically *de novo* (Figures 7 and 8). All chemicals were of reagent grade and

purchased from Sigma-Aldrich (St Louis, MO). Separation of the compounds by column

chromatography was carried out with silica gel 60 (200−300 mesh ASTM, E. Merck, Germany).

The quantity of silica gel used was 50–100 fold the weight of the column. TLC was based on

silica gel-coated aluminum sheets (silica gel 60 GF254, E. Merck) and visualized under UV

light (254 nm). ^{1}H NMR and ^{13}C NMR spectra were recorded on a Bruker model digital

AVANCE III 400 MHz and 700 MHz spectrometer (Kontich, Belgium) at 25 °C using TMS

as an internal standard. Chemical shifts were recorded as δ values in ppm and were indirectly

referenced to TMS by the solvent signal. *J* is reported in Hz.
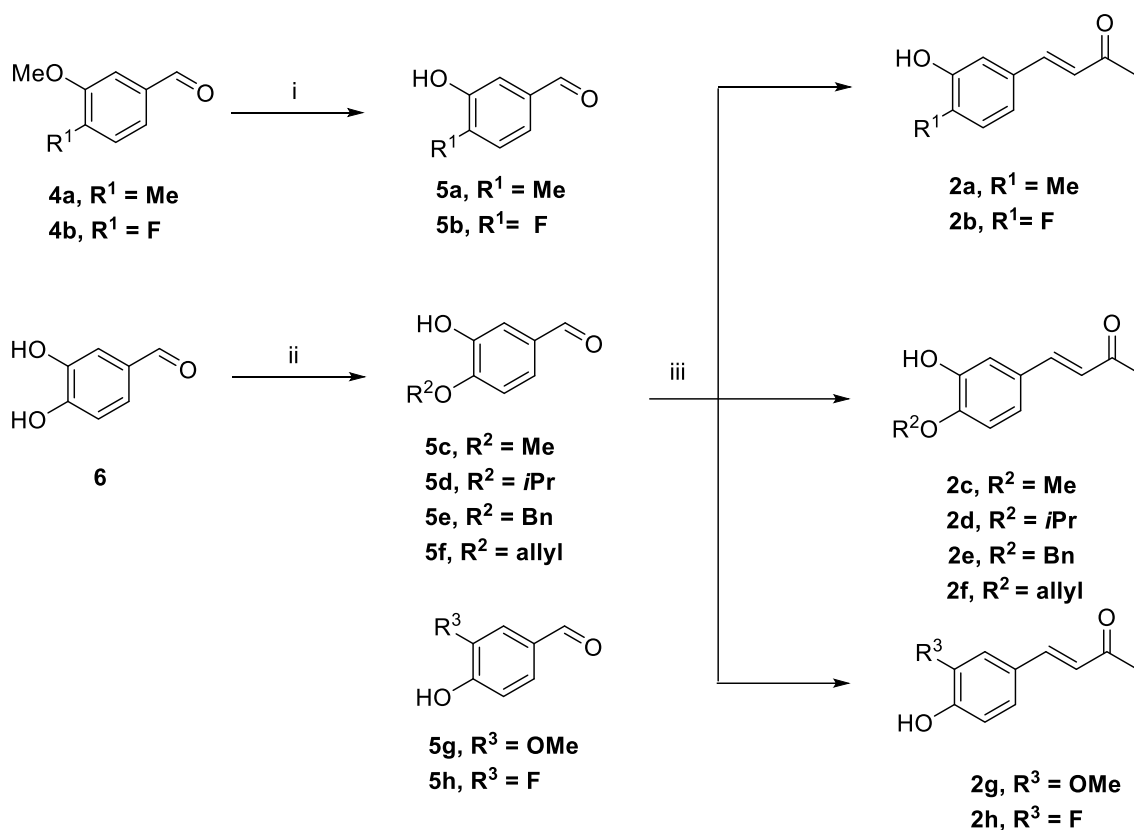
Figure 7. Scheme 1. Reagents and conditions: (i) BBr₃, DCM, -10 °C to rt, 6 h, 41 ~ 53%; (ii) alkyl bromide, K₂CO₃, DMF, 70 °C, overnight, 50 ~ 65%; (iii) CuBr₂, acetone, 60 °C, 6 h; 12 ~ 42%.
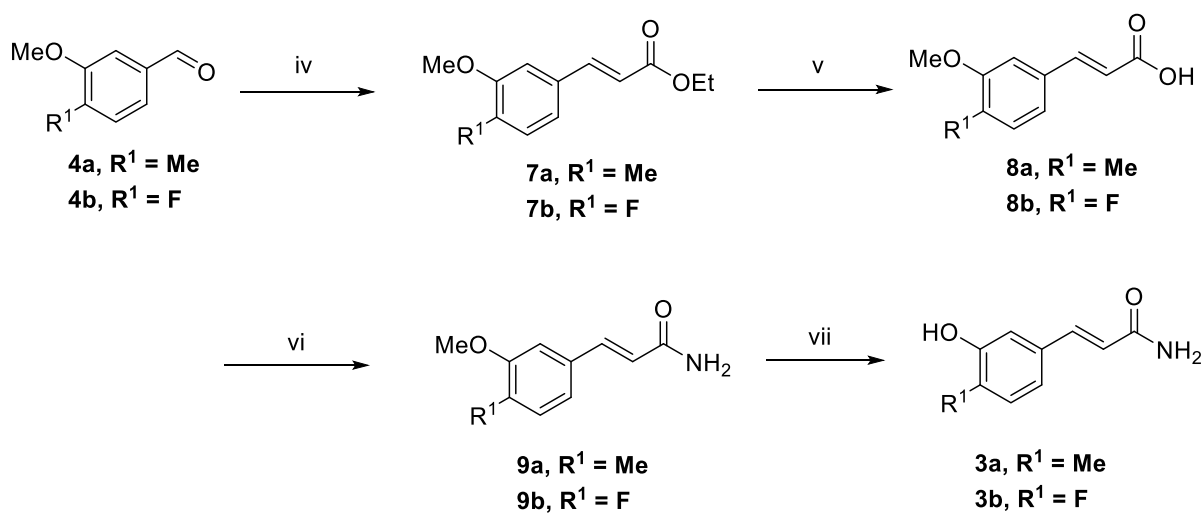

Figure 8. Scheme 2. Reagents and conditions: (iv) 60% NaH, triethyl phosphonoacetate, THF, rt, 20 h, 60 ~ 63%; (v) 2 N NaOH (aq), THF, reflux, 2 h, 93 ~ 98%; (vi) (Boc)₂O, pyridine,

NH$_4$HCO$_3$, dioxane, 60 °C, 2 h, 40 ~ 68%; (vii) BBr$_3$, DCM, -10 °C to rt, 6 h, 40 ~ 48.3%.

Representative Compounds and Synthesis Procedures. All of the compounds were synthesized via scheme 1 (compounds **2a−h**) (Figure 7) and scheme 2 (compounds **3a and b**) (Figure 8) except commercially available compounds (Figure 1).

Representative Syntheses of (*E*)-4-(Substituted-phenyl)but-3-en-2-one Derivatives (2a−h). Arylaldehyde (1.0 mmol) and CuBr$_2$ (1.0 mmol) in a pressured tube were dissolved in 5 mL acetone at rt. The reaction mixture was stirred at 60 °C. After 6 h, the mixture was cooled to rt, and filtered with Celite. The organic layer was concentrated *in vacuo*, and the product was purified by flash chromatography using ethyl acetate and *n*-hexane (1:4) as an eluent.

(*E*)-4-(3-Hydroxy-4-methylphenyl)but-3-en-2-one (2a). This compound was isolated as a brown solid (17%); ^{1}H NMR (700 MHz, CD$_3$OD): δ 7.56 (1H, d, *J* = 16.24 Hz), 7.14 (1H, d, *J* = 7.42 Hz), 7.03 – 7.02 (2H, m), 6.67 (1H, *J* = 16.24 Hz), 2.38 (3H, s), 2.22 (3H, s); ^{13}C NMR (175 MHz, MeOD) δ 200.08, 155.71, 144.92, 133.18, 130.86, 128.18, 125.28, 120.14, 112.92, 25.72, 14.92); Ms(ESI) *m/z* : 177. [M+H]$^+$.

(*E*)-4-(4-Fluoro-3-hydroxyphenyl)but-3-en-2-one (2b). This compound was isolated as a yellow solid (12%); ^{1}H NMR (400 MHz, CD$_3$OD): δ 7.56 (1H, d, *J* = 16.4 Hz), 7.22 (1H, dd, *J* = 7.6, 2.1 Hz), 7.13 – 7.10 (2H, m), 6.67 (1H, *J* = 16.4 Hz), 2.38 (3H, s); ^{13}C NMR (175 MHz, MeOD) δ 199.78, 153.84, 152.44, 145.43, 145.36, 143.51, 131.34, 131.32, 126.12, 126.11, 120.51, 120.47, 116.65, 116.63, 116.10, 115.99, 25.85; Ms(ESI) *m/z* : 181.1 [M+H]$^+$.

(*E*)-4-(3-Hydroxy-4-methoxyphenyl)but-3-en-2-one (2c). This compound was isolated as a yellow solid (47.8%); ^{1}H NMR (400 MHz, DMSO): δ 9.22 (1H, br), 7.48 (1H, d, *J* = 16.4 Hz), 7.14 – 7.10 (2H, m), 6.97 (1H, d, *J* = 8.0 Hz), 6.54 (1H, *J* = 16.4 Hz), 3.81 (3H, s), 2.29(3H, s); ^{13}C NMR (175 MHz, CDCl$_3$) δ 198.62, 148.86, 145.99, 143.56, 127.96, 125.44, 122.15, 113.23, 110.66, 56.03, 27.46; Ms(ESI) m/z : 193.1 [M+H]$^+$.

(*E*)-4-(3-Hydroxy-4-isopropoxyphenyl)but-3-en-2-one (2d). This compound was isolated as a brown solid (70%); ^{1}H NMR (400 MHz, CDCl$_3$) δ 7.44 (1H, d, *J* = 16.0 Hz), 7.17 (1H, d, *J* = 2.4 Hz), 7.05 (1H, dd, *J* = 8.4 Hz, 6.0 Hz), 6.87 (1H, d, *J* = 8.4 Hz), 6.60 (1H, d, *J* = 16.0 Hz), 5.74 (1H, s), 4.67 (1H, hept, *J* = 6.4 Hz), 2.37 (3H, s), 1.41 (6H, d, *J* = 6.0 Hz); ^{13}C NMR (175 MHz, CDCl$_3$) δ 198.50, 146.95, 146.70, 143.51, 127.71, 125.39, 121.94, 113.31, 112.66, 71.75, 29.71, 27.49, 22.09; Ms(ESI) *m/z* : 221.1 [M+H]$^+$.

(*E*)-4-(4-Benzyloxy-3-hydroxyphenyl)but-3-en-2-one (2e). This compound was isolated as a yellow solid (40%); ^{1}H NMR (400 MHz, CDCl$_3$) δ 7.46 – 7.42 (6H, m), 7.19 (1H, d, *J* = 2.0 Hz), 7.05 (1H, dd, *J* = 8.4 Hz, 2.4 Hz), 6.95 (1H, d, *J* = 8.4 Hz), 6.95 (1H, d, *J* = 8.4 Hz), 6.61 (1H, d, *J* = 16.0 Hz), 5.71 (1H, s), 5.17 (2H, s), 2.37 (3H, s); ^{13}C NMR (175 MHz, CDCl$_3$) δ 198.45, 147.91, 146.16, 143.31, 135.69, 128.86, 128.68, 128.33, 127.89, 125.65, 121.98, 113.45, 112.03, 71.18, 27.54; Ms(ESI) *m/z* : 269.2 [M+H]$^+$.

(*E*)-4-(4-Allyloxy-3-hydroxyphenyl)but-3-en-2-one (2f). This compound was isolated as a yellow solid (56%); ^{1}H NMR (400 MHz, CDCl$_3$) δ 7.43 (1H, d, *J* = 16.4 Hz), 7.18 (1H, d, *J* = 2.4 Hz), 7.04 (1H, dd, *J* = 8.4 Hz, 2.0 Hz), 6.87 (1H, d, *J* = 8.0 Hz), 6.60 (1H, d, *J* = 16.0 Hz), 6.11 – 6.04 (1H, m), 5.80 (1H, s), 5.43 (1H, dd, *J* = 17.2 Hz, 12.8 Hz), 5.36 (1H, dd, *J* = 10.4 Hz, 8.0 Hz), 4.67 – 4.65 (2H, m), 2.37 (3H, s); ^{13}C NMR (175 MHz, CDCl$_3$) δ 198.54, 147.76, 146.16, 143.44, 132.27, 128.17, 125.56, 121.96, 118.89, 113.47, 111.99, 69.85, 27.50; Ms(ESI) *m/z* : 219.2 [M+H]$^+$.

(*E*)-4-(4-Hydroxy-3-methoxyphenyl)but-3-en-2-one (2g). This compound was isolated as a yellow solid (42%); ^{1}H NMR (400 MHz, DMSO): δ 7.52 (1H, d, *J* = 16.4 Hz), 7.29 (1H, d, *J* = 2.0 Hz), 7.13 (1H, dd, *J* = 1.6, 2.0 Hz), 6.80 (1H, *J* = 8.0 Hz), 6.67 (1H, *J* = 16.4 Hz), 3.81 (3H, s), 2.28(3H, s); ^{13}C NMR (175 MHz, CDCl$_3$) δ 198.60, 148.33, 146.93, 143.90, 126.89, 124.95, 123.56, 114.86, 109.36, 55.97, 27.29; Ms(ESI) *m/z* : 193.1 [M+H]$^+$.

(*E*)-4-(3-Fluoro-4-hydroxyphenyl)but-3-en-2-one (2h). This compound was isolated as a yellow solid (24.4%); ^{1}H NMR (400 MHz, DMSO): δ 7.58 (1H, dd, *J* = 2.0, 2.0 Hz), 7.51 (1H, d, *J* = 16.4 Hz), 7.35 (1H, dd, *J* = 1.6, 1.6 Hz), 6.97 (1H, t, *J* = 8.8 Hz), 6.66 (1H, *J* = 16.4 Hz), 2.28 (3H, s); ^{13}C NMR (175 MHz, CDCl$_3$) δ 199.30, 151.99, 150.63, 146.47, 146.38, 143.07, 125.98, 125.97, 125.67, 117.96, 117.94, 115.06, 114.96, 27.45; Ms(ESI) *m/z* : 181.1 [M+H]$^+$.

(*E*)-3-(3-Hydroxy-4-methylphenyl)acrylamide (3a). Boron tribromide (1 M methylene chloride solution, 1.04 mL) was gradually added dropwise to a methylene chloride (1 mL) solution of (*E*)-3-(3-methoxy-4-methylphenyl)acrylamide (**9a**) (40 mg, 0.21 mmol) under ice cooling. The reaction solution was agitated at rt for 4 h after the additions ended. The reaction solution was again cooled with ice, iced water was gradually added to the reaction solution to terminate the reaction, and further 5 N hydrochloride solution was added until pH 1. After condensing the reaction solution under reduced pressure, water and ethyl acetate were added to the residue, and the organic layer was separated. The organic layer obtained was washed with a saturated sodium chloride solution, and the solvent was evaporated under reduced pressure after drying over anhydrous magnesium sulfate. The residue obtained was purified by silica gel column chromatography (elution solvent: methylene chloride/MeOH 20:1) to produce (*E*)-3-(3-hydroxy-4-methylphenyl)acrylamide (**3a**) (18 mg, 48.3%) as a yellow solid. ^{1}H NMR (400 MHz, MeOD): δ 7.45 (1H, d, *J* = 15.6 Hz), 7.10 (1H, d, *J* = 7.6 Hz), 6.98-6.95 (2H, m), 6.53 (1H, *J* = 15.6 Hz), 2.13 (3H, s); ^{13}C NMR (175 MHz, MeOD) δ 169.90, 155.57, 141.72, 133.49, 130.75, 126.96, 119.02, 118.58, 113.08, 14.83; Ms(ESI) *m/z* : 178.1 [M+H]$^+$.

(*E*)-3-(4-Fluoro-3-hydroxyphenyl)acrylamide (3b). Boron tribromide (1 M methylene chloride solution, 1.1 mL) was gradually added dropwise to a methylene chloride (1 mL) solution of (*E*)-3-(4-fluoro-3-methoxyphenyl)acrylamide (**9b**) (43 mg, 0.22 mmol) under ice cooling. The reaction solution was agitated at rt for 4 h after the additions ended. The reaction

solution was again cooled with ice, iced water was gradually added to the reaction solution to terminate the reaction, and further 5 N hydrochloride solution was added until pH 1. After condensing the reaction solution under reduced pressure, water and ethyl acetate were added to the residue, and the organic layer was separated. The organic layer obtained was washed with a saturated sodium chloride solution, and the solvent was evaporated under reduced pressure after drying over anhydrous magnesium sulfate. The residue obtained was purified by silica gel column chromatography (elution solvent: methylene chloride/MeOH 20:1) to produce (*E*)-3-(4-fluoro-3-hydroxyphenyl)acrylamide (**3b**) (16 mg, 40%) as a yellow solid. ^{1}H NMR (400 MHz, MeOD): δ 7.45 (1H, d, *J* = 12.4 Hz), 7.15 (1H, dd, *J* = 2.0, 2.0 Hz), 7.10-7.01 (2H, m), 6.52 (1H, d, *J* = 16.0 Hz); ^{13}C NMR (175 MHz, MeOD) δ 169.55, 153.34, 151.95, 145.27, 145.20, 140.62, 131.58, 131.56, 119.66, 119.63, 119.50, 119.49, 116.33, 116.31, 115.97, 115.86; Ms(ESI) *m/z* : 193.1 [M+H]$^{+}$.

General Demethylation for 3-Hydroxy-4-substituted Benzaldehydes (5a and 5b). Boron tribromide (1 M methylene chloride solution, 5 mL) was added dropwise to a methylene chloride (5 mL) solution of 3-methoxy-4-substituted benzaldehyde, (**4a**) (Santa Cruz Biotechnology, Dallas, TX) and (**4b**) (Sigma-Aldrich) (2.66 mmol, respectively), under ice-cooling. The reaction solution was agitated at rt for 5 h after the addition. The reaction solution was again cooled with ice. Iced water was gradually added to the reaction solution to terminate the reaction, followed by additional 5 N hydrochloride solution until the pH reached 1. After condensing the reaction solution under reduced pressure, water and ethyl acetate were added to the residue, and the organic layer was separated. The resulting organic layer was washed with saturated sodium chloride solution, and the solvent was evaporated under reduced pressure after drying over anhydrous magnesium sulfate. The residue obtained was purified by silica gel column chromatography (elution solvent: n-hexane/ethyl acetate 4:1), and the desired compounds **5a** and **5b** were obtained. 3-Hydroxy-4-methylbenzaldehyde (**5a**) was reacted from

3-methoxy-4-methylbenzaldehyde (**4a**) (400 mg, 2.66 mmol), isolated as a solid (150 mg, 41.4%). 4-Fluoro-3-hydroxybenzaldehyde (**5b**) was reacted from 4-fluoro-3-methoxybenzaldehyde (4b) (410 mg, 2.66 mmol), isolated as a solid (148 mg, 39.7%).

General Alkylation of 3-Hydroxy-4-substituted Benzaldehydes (5c-h). A stirred suspension of 3,4-dihydroxybenzaldehyde (**6**) (Sigma-Aldrich) (250 mg, 1.81 mmol) and anhydrous potassium carbonate (250 mg, 1.81 mmol) in dry DMF (3 mL) was heated to 70 ºC, and alkyl or alkenyl bromide (1 equiv) was added dropwise under nitrogen over 30 min. The mixture was stirred overnight at rt and then poured into iced water (50 mL). The aqueous mixture was extracted with ethyl acetate, and the combined extracts were washed with water, brine, and evaporated under vacuum to yield brown oil. The residue was purified by silica gel column chromatography (ethyl acetate/*n*-hexane 1:4), and the product **5c-5f** (38~50%) were obtained as solids. 3-hydroxy-4-methoxybenzaldehyde (**5c**) was reacted with methyl iodide (257 mg, 1.81 mmol), isolated as a solid (72 mg, 48%). 3-Hydroxy-4-isopropoxybenzaldehyde (**5d**) was reacted with 2-bromopropane (223 mg, 1.81 mmol), isolated as a solid (46 mg, 50%). 4-(Benzyloxy)-3-hydroxybenzaldehyde (**5e**) was reacted with benzyl bromide (310 mg, 1.81 mmol), isolated as a solid (95 mg, 41%). 4-(Allyloxy)-3-hydroxybenzaldehyde (**5f**) was reacted with allyl bromide (219 mg, 1.81 mmol), isolated as a solid (80 mg, 45%). Compounds **5g** (Sigma-Aldrich) and **5h** (Sigma-Aldrich) for syntheses of compounds **2g** and **2h** were commercially available, used without further purification.

Ethyl-(*E*)-3-(3-methoxy-4-methylphenyl)acrylate (7a). Sodium hydride (60% dispersion oil prewashed in hexane, 300 mg, 7.5 mmol) was stirred in dry THF (10 mL) under 1 atm of nitrogen. Triethyl phosphonoacetate (1.345 g, 6 mmol) in dry THF (3 mL) was added dropwise and stirred for 25 min. Then, 3-methoxy-4-methylbenzaldehyde (**4a**) (Santa Cruz Biotechnology) (751 mg, 5 mmol) in THF (3 mL) was added dropwise over a period of approximately 30 min (in order to prevent a gum like precipitate that had previously been

observed). The resulting solution was stirred for 20 h at rt. The reaction mixture was then quenched with water (100 mL) and extracted with ethyl acetate (3 × 100 mL). The combined organic extracts were dried over magnesium sulfate, filtered and concentrated *in vacuo*. Purification by flash column chromatography (ethyl acetate/*n*-hexane 1:4) afforded unsaturated ester **7a** (700 mg, 63%) as a yellow oil.

Ethyl (*E*)-3-(4-fluoro-3-methoxyphenyl)acrylate (7b). Sodium hydride (60% dispersion oil prewashed in hexane, 300 mg, 7.5 mmol) was stirred in dry THF (10 mL) under 1 atm of nitrogen. Triethyl phosphonoacetate (1.345 g, 6 mmol) in dry THF (3 mL) was added dropwise and stirred for 25 min. Then 4-fluoro-3-methoxybenzaldehyde (**4b**) (Sigma-Aldrich) (770.7 mg, 5 mmol) in THF (3 mL) was added dropwise over a period of approximately 30 min (in order to prevent a gum like precipitate that had previously been observed). The resulting solution was stirred for 20 h at rt. The reaction mixture was then quenched with water (100 mL) and extracted with ethyl acetate (3 × 100 mL). The combined organic extracts were dried over magnesium sulfate, filtered and concentrated *in vacuo*. Purification by flash column chromatography (ethyl acetate/*n*-hexane 1:4) afforded unsaturated ester **7b** (680 mg, 60.6%) as a yellow oil.

(*E*)-3-(3-Methoxy-4-methylphenyl)acrylic acid (8a). Ethyl (*E*)-3-(3-methoxy-4-methylphenyl)acrylate (**7a**) (220 mg, 1 mmol) dissolved in THF (5 mL) was added dropwise to sodium hydroxide (2.0 M, 5 mL) and heated to reflux for 2 h. The mixture was quenched with water (10 mL) and acidified to pH 2 with hydrochloric acid (2.0 M). The solution was then extracted with ethyl acetate (3 × 100 mL), dried over sodium sulfate, filtered and concentrated *in vacuo* to yield (190 mg, 98.8%) as a white solid.

(*E*)-3-(4-Fluoro-3-methoxyphenyl)acrylic acid (8b). Ethyl (*E*)-3-(4-fluoro-3-methoxyphenyl)acrylate (**7b**) (224 mg, 1 mmol) dissolved in THF (5 mL) was added dropwise

to sodium hydroxide (2.0 M, 5 mL) and heated to reflux for 2 h. The mixture was quenched

with water (10 mL) and acidified to pH 2 with hydrochloric acid (2.0 M). The solution was

then extracted with ethyl acetate (3 × 100 mL), dried over sodium sulfate, filtered and

concentrated *in vacuo* to yield (183 mg, 93.2%) as a white solid.

(*E*)-3-(3-Methoxy-4-methylphenyl)acrylamide (9a). To a solution of (*E*)-3-(3-methoxy-4-

methylphenyl)acrylic acid (**8a**) (100 mg, 0.52 mmol) and pyridine (0.1 mL) in dioxane (1 mL),

was added di-tert-butyl dicarbonate (227 mg, 1.04 mmol) in one portion followed by

ammonium bicarbonate (83 mg, 1.04 mmol) in one portion, and the mixture was stirred at 60

ᵒC for 2 h. The reaction mixture was concentrated *in vacuo* and the residue was partitioned

between ethyl acetate and water. The ethyl acetate phase was washed with 5% aqueous sodium

bicarbonate, 0.1 N HCl and brine. The organic phase was dried over sodium sulfate, filtered

and concentrated *in vacuo* to **9a** (68 mg, 68.3%) as a yellow solid, and used without further

purification.

(*E*)-3-(4-Fluoro-3-methoxyphenyl)acrylamide (9b). To a solution of (*E*)-3-(4-fluoro-3-

methoxyphenyl)acrylic acid (**8b**) (100 mg, 0.51 mmol) and pyridine (0.1 mL) in dioxane (1

mL) was added di-tert-butyl dicarbonate (225 mg, 1.02 mmol) in one portion followed by

ammonium bicarbonate (82 mg, 1.02 mmol) in one portion, and the mixture was stirred at 60

ᵒC for 2 h. The reaction mixture was concentrated *in vacuo* and the residue was partitioned

between ethyl acetate and water. The ethyl acetate phase was washed with 5% aqueous sodium

bicarbonate, 0.1 N HCl and brine. The organic phase was dried over sodium sulfate, filtered

and concentrated *in vacuo* to **9b** (53 mg, 53.2%) as a yellow solid, and used without further

purification.

Purity Determination of Compounds 2a−h and 3a, b. For qualitative analysis, an Agilent

1200 series HPLC instrument (Agilent Technologies, Inc. Santa Clara, CA) composed of an

online degasser (G1322A), a quaternary pump (G1312A), an autosampler (G1367C), a column

temperature controller (G1316A), and a DAD (G1315B) was used. Analyses were carried out

on a Waters TC-C18 reversed-phase analytical column (2.1 × 50 mm, 2 μm) (Waters Co.,

Milford, MA) at a flow rate of 0.3 mL/min. The detection wavelength was set at 250 nm. The

injection volume was 2 μL, and the column temperature was maintained at 40 °C. The mobile

phase consisted of the solvent A (0.1%, v/v solution of formic acid in water) and solvent B

(0.1%, v/v solution of formic acid in acetonitrile) filtered through a 0.45 μm membrane filter,

and was subject to gradient elution (0.00 min: solvent A 90%, solvent B 10%. 0.50 min: solvent

A 90%, solvent B 10%. 2.50 min: solvent A 0%, solvent B 100%. 3.50 min: solvent A 0%,

solvent B 100%. 5.00 min: solvent A 90%, solvent B 10%. 6.00 min: solvent A 90%, solvent

B 10%). As a result, ≥95% purity was confirmed for each compound tested. Purity and NMR

data of the synthesized compounds are presented in Supporting Information 1, 2.

Cell Culture. MC3T3-E1 subclone 4 murine osteoblastic cells (#CRL-2593TM, ATCC)

were cultured in minimum essential medium Eagle-Alpha modification (α-MEM; #LM00853,

WELGENE, Seoul, Korea) at 37 °C under 5% CO_2 tension. HaCaT human epidermal

keratinocytes (#ATCC PCS-200-011) were cultured in Dulbecco's modified Eagle's medium

(DMEM; #DMEM-HPA, Capricorn Scientific, Ebsdorfergrund, Germany) at 37 °C under 5%

CO_2 tension. NIH3T3 mouse embryo fibroblast (#KCLB 21658), RAW264.7 murine

macrophage (preosteoclast cell line) (#KCLB 40071), HCT116 human colon carcinoma

(#KCLB 10247), PC3 human prostate adenocarcinoma (#KCLB 21435), HT1080 human

fibrosarcoma (#KCLB 10121), and B16F10 mouse melanoma cells (#KCLB 80008) were

purchased from Korean Cell Line Bank, Seoul, Korea, and cultured in DMEM at 37 °C under

5% CO_2 tension. AGS human stomach adenocarcinoma (#KCLB 21739), A549 human lung

carcinoma (#KCLB 10185), Caki-1 human kidney carcinoma (#KCLB 30046), T24 human

bladder carcinoma (#KCLB 30004), and TC-1 P3 HPV-16 E7-expressing mouse lung epithelial

cells (- MHC class I) (kindly donated by professor Tae Woo Kim, Department of Biochemistry and Molecular Biology, College of Medicine, Korea University, Seoul, Korea) were cultured in RPMI-1640 (#RPMI-A, Capricorn Scientific) at 37 °C under 5% CO_2 tension. Human adipose-derived mesenchymal stem cells (ADMSCs; CEFO Bio, Seoul, Korea) were cultured in CB-ADMSC-GM (CEFO Bio) at 37 °C under 5% CO_2 tension.

Animal. For BMM preparation, animal experiments were performed with approval of the regulatory committee of College of Medicine, Korea University (KOREA-2016-0148) in compliance with institutional guidelines. Male C57BL/6 mice (4-week old) were purchased from Orientbio (Seoul, Korea), acclimated for a week, and euthanized using CO_2 chamber (JEUNG DO BIO & PLANT Co., LTD, Seoul, Korea) to extract BMM from femur and tibia. Pharmacokinetic study was approved by the Institutional Animal Care and Use Committee (IACUC) of Korea Research Institute of Chemical Technology. Six-week-old male ICR mice obtained from Korea Research Institute of Chemical Technology (Daejeon, Korea) were used. Mice were housed in facilities at the Laboratory Animal Research Center, Korea Research of Chemical Technology, and maintained at $25 \pm 2°C$ and $60 \pm 10\%$ relative humidity in 12 h light/dark cycle. OVX-induced osteoporosis experiment was performed with approval of the regulatory committee of College of Medicine, Korea University (KOREA-2018-0088) in compliance with institutional guidelines. Female ddY mice (4-week old) were purchased from Orientbio, and acclimated for a week.

Primary Culture and Induction of Osteoclastogenesis of Murine BMM. Bone marrow cells were collected from femurs and tibias of 5-to 8-week-old male C57BL/6 mice. The bones were stripped of muscle and stored in ice-cold PBS (#CAP08-050, GenDEPOT, Katy, TX). Both ends of each bone were cut, and the bone marrow was flushed with ice-cold flushing media (serum-free α-MEM, 2 mM EDTA) using a 25G needle. Bone marrow cells were collected by centrifugation at 3,000 rpm for 3 min in Labogene 1248R (Labogene, Lynge,

Denmark), and then resuspended in flushing media. To separate mononuclear cells, 8 mL of bone marrow cell suspension was overlaid on top of 6 mL of Lymphocyte Separation Medium (LSM) (#50494, MP Biomedicals, Santa Ana, CA), and centrifuged at 1,600 rpm for 20 min in Labogene 1248R (Labogene). The band of BMM at the media interface was collected, and 1×10^5 cells were cultured in 0.5 mL of complete α-MEM containing 10% fetal bovine serum (FBS; Capricorn Scientific) and 1% (v/v) of antibiotics (100 U/mL penicillin G and 100 mg/mL streptomycin) per well, in a 48-well plate at 37 °C under 5% CO_2 tension with media changed on day 3. To promote osteoclast differentiation, cells were grown in the presence of osteoclast differentiation factors, M-CSF (60 ng/mL) (PeproTech, Seoul, Korea) and RANKL (150 ng/mL) (PeproTech). Macrophage/monocyte lineage cells were fully differentiated into mature multinucleated osteoclasts after 6 d.[62] Multinucleated osteoclasts were identified by TRAP staining performed according to the manufacturer's instructions (Sigma-Aldrich). TRAP+ multinucleated cells were counted as fully differentiated osteoclasts. As a negative control, cells were cultured in the presence of M-CSF (60 ng/mL) only. IC_{50} was defined as the concentration that induced 50% reduction of TRAP+ multinucleated cells. Representative images of cells on an inverted microscope (Nikon ECLIPSE Ti-U, Nikon, Melville, NY) were captured using Imaging Software NIS-Elements F Ver4.60.00 for 64bit edition (Nikon) at 40 × magnification.

Determination of IC_{50} of Benzylideneacetone Derivatives to Inhibit Osteoclastogenesis.
Compound **1** (Alfa Aesar, Thermo Fisher Scientific, Haverhill, MA), natural benzylideneacetone derivatives including compound **2g** (Sigma-Aldrich), protocatechualdehyde (Sigma-Aldrich), (*E*)-4-hydroxybenzalacetone (ACROS ORGANICS, Thermo Fisher Scientific, Geel, Belgium), caffeic acid (Sigma-Aldrich), neochlorogenic acid (Sigma-Aldrich), chlorogenic acid (CarlRoth, Karlsruhe, Germany), protocatechuic acid (Sigma-Aldrich), protocatechuic acid methyl ester (Alfa Aesar), homoprotocatechuic acid

(Sigma-Aldrich), homoprotocatechuic acid methyl ester (Alfa Aesar), *trans*-cinnamic acid (Sigma-Aldrich), and phenylacetic acid (Sigma-Aldrich), and synthetic benzylideneacetone derivatives including (*E*)-4-(3-hydroxy-4-methylphenyl)-3-buten-2-one (**2a**), (*E*)-4-(4-fluoro-3-hydroxyphenyl)-3-buten-2-one (**2b**), compound **2c** (Specs, Zoetermeer, The Netherlands), (*E*)-4-(3-hydroxy-4-isopropoxyphenyl)but-3-en-2-one (**2d**), (*E*)-4-(4-benzyloxy-3-hydroxyphenyl)but-3-en-2-one (**2e**), (*E*)-4-(4-allyloxy-3-hydroxyphenyl)but-3-en-2-one (**2f**), (*E*)-4-(3-fluoro-4-hydroxyphenyl)-3-buten-2-one (**2h**), (*E*)-4-(3-hydroxy-4-methylphenyl)acrylamide (**3a**), and (*E*)-4-(4-fluoro-3-hydroxyphenyl)acrylamide (**3b**) (Figure 1) were dissolved in DMSO. Alendronate (Cayman, Ann Arbor, MI), used as a reference compound, was dissolved in PBS. To determine IC_{50} to inhibit osteoclastogenesis, each compound was added at a range of concentrations $0.01-100\,\mu M$. C57BL/6 BMM (1×10^5 cells) prepared as described previously were cultured in 0.5 mL of complete α-MEM per well in a 48-well plate in the presence of M-CSF (60 ng/mL) and RANKL (150 ng/mL) at 37 ^oC under 5% CO_2 tension for 6 d with a media change on day 3. As a negative control, the cells were cultured in the presence of M-CSF (60 ng/mL) only. On the sixth day after the induction of differentiation, multinucleated mature osteoclasts were identified by TRAP staining performed according to the manufacturer's instructions (Sigma-Aldrich). TRAP+ multinucleated cells were counted as fully differentiated osteoclasts on an inverted microscope (Nikon ECLIPSE Ti-U, Nikon). IC_{50} was defined as the concentration that induced 50% reduction of the number of TRAP+ multinucleated cells.

Co-Culture of Preosteoclast and Preosteoblast. C57BL/6 BMM (1×10^5) prepared as described previously and MC3T3-E1 murine osteoblastic cells (1.5×10^4) were co-cultured in 500 µL of complete α-MEM per well in 48-well plate at 37 ^oC under 5% CO_2 tension with media changes every 3-4 d. Positive control cells were grown in the presence of osteoclast differentiation factors, M-CSF (60 ng/mL) and RANKL (150 ng/mL), and osteoblast

differentiation factors, ascorbic acid (50 µg/mL) and 10 mM β–glycerophosphate. Negative

control cells were grown in the presence of M-CSF only. To test the effect of compound **1** on

the differentiation of osteoclast and osteoblast, compound **1** was administered to the co-culture

to a final concentration of 10 µM. Cells were cultured for 21 d. On the sixth day after the

induction of differentiation, representative images of co-cultured cells on an inverted

microscope (Nikon ECLIPSE Ti-U) were captured using Imaging Software NIS-Elements F

Ver4.60.00 for 64bit edition (Nikon) at 40 × magnification.

Bone Resorption Assay. *In vitro* osteoclast-mediated degradation of human bone collagen

was measured using the OsteoLyse[TM] Assay Kit (Lonza Walkersville, Inc. Walkersville, MD)

according to the manufacturer's instructions. The assay directly measured the release of matrix

metalloproteinases into the resorption lacuna of the osteoclasts.[63] Briefly, 2×10^4 BMM

prepared as previously described were seeded onto the 96-well OsteoLyse[TM] Cell Culture Plate

coated with fluorophore-derivatized human bone matrix (europium-conjugated collagen) in

100 µL of complete α-MEM per well in the presence of M-CSF (60 ng/mL) and RANKL (150

ng/mL), and incubated for 6 d in a 5% CO_2 incubator at 37 °C with the media replaced on day

3 after seeding. To measure the capacity of compound **1** to inhibit the osteolytic function of

mature osteoclasts, compound **1** was added at a concentration of IC_{50}, 7.8 µM, with a media

change at day 6. After treating mature osteoclasts with compound **1** for 3 d, 10 µL of cell

culture supernatants were taken and added to fluorophore-releasing reagents in a second 96-

well assay plate, and assessed for the degraded collagen in a time-resolved fluorescence

fluorimeter (Wallac Victor, Perkin Elmer, Waltham, MA), with excitation at 340 nm and

emission at 615 nm over a 400 µs time period after an initial delay of 400 µs. The proportion

of bone resorption was calculated as the ratio of the amount of bone resorption in the presence

of compound **1** to that of the untreated control, and normalized by cellular DNA. Three

experiments were conducted to obtain mean ± SD.

ALP Activity Assay. ALP activity was determined as described with minor modifications.[64] Briefly, 3×10^3 MC3T3-E1 murine osteoblastic cells were cultured in 100 µL of complete α-MEM with ascorbic acid (50 µg/mL) and 10 mM β-glycerophosphate per well in 96-well plate in the presence of benzylideneacetone derivatives (10 and 50 µM) or PTH-related protein (Bachem. Bubendorf, Switzerland) dissolved in PBS to a final concentration of 1 µM and used as a reference compound in a 5% CO_2 incubator at 37 °C. Media were changed every 3-4 d. On day 14, cells were washed with PBS, and sonicated with a sonic dismembrator model 500 (ThermoFisher Scientific Korea, Seoul, Korea) at 4 °C. Sonicated lysates were centrifuged for 10 min at $1,500 \times$ g, and the supernatants were subject to ALP assay. ALP activities were measured using Quantichrom ALP Assay Kit (Bioassay Systems, Hayward, CA) according to the manufacturer's instructions. ALP activity was measured with a plate reader (Molecular Devices, Sunnyvale, CA) at 405 nm. The % activation of ALP activity represents ALP activity of cells treated with a test compound compared with that of untreated control cells. Results were normalized by cellular protein using Pierce™ BCA Protein Assay Kit (Thermo Scientific, Rockford, IL).

Western Blot Analysis. Cells were lysed in RIPA buffer (Biosesang, Seoul, Korea). Protein concentration was determined using Pierce™ BCA Protein Assay Kit (Thermo Scientific). Proteins were resolved by SDS-PAGE on 12.5% polyvinylidene-Tris gels and transferred electrophoretically onto polyvinylidene difluoride (PVDF) membrane. Membranes were blocked with skim milk and probed with anti-NF-kB p65 (C-20) antibody (#sc-372, Santa Cruz Biotechnology, Dallas, TX), anti-NFATc1 polyclonal antibody (Isotype: IgG. Host: rabbit) (#MBS127656, MyBioSource Korea, Seoul, Korea), anti-RUNX2 (D1H7) rabbit monoclonal antibody (#8486, Cell Signaling Technology, MA), or anti-OCN (FL-95) antibody (#sc-30045, Santa Cruz Biotechnology), respectively. Anti-actin antibody (#M177-3, MEDICAL &

BIOLOGICAL LABORATORIES CO. LTD. Nagoya, Japan) was used as an internal standard. Protein bands on blots were visualized using enhanced chemiluminescent detection kit (PicoEPD Western Reagent, ELPIS-BIOTECH, Daejeon, Korea) and MICROCHEMI DNr (Bio-Imaging Systems, Neve Yamin, Israel). Band density was quantitated using ImageJ 1.51k downloaded from Wayne Rasband National Institutes of Health, USA (http://imagej.nih.gov/ij).

Pharmacokinetic Study. Compounds **1** and **2c** were dissolved with DMSO, and diluted with distilled water (DW) and PEG400 (DMSO:DW:PEG400 = 5:55:40), respectively. Each compound was administered to three ICR mice in IV (2 mg/kg) injection through a tail vein and PO (10 and 50 mg/kg) using gavage. After administration, blood samples were collected from the retro-orbital venous sinus at 0.00, 0.08, 0.25, 0.75, 1, 2, 3, 4, 6, 8 h, and centrifuged to obtain plasma. The plasma was added with a 0.1 M PBS buffer pH 7.4 (1:1) and an internal standard substance, and subjected to solid phase extract (SPE) using Oasis HLB 96-well µElution plate containing a reversed-phase sorbent (Waters Co.) for cleanup and analyte enrichment according to manufacturer's instructions. Compounds **1** and **2c** extracted were analyzed for their concentrations by LC-MS/MS with HPLC (Agilent 1260, Agilent Technologies, Inc.) equipped with a reverse phase column and Mass Spectrometry (Agilent 6460, Agilent Technologies, Inc.). Non-compartmental pharmacokinetic parameters were calculated from the blood concentration-time plots of the compounds, using non-compartmental analysis model of Phoenix® WinNonlin™ 6.4 (Pharsight, Certara®, Cary, NC).

Surgical Procedure for OVX. Four 5-week-old female ddY mice per group with similar body weights were selected. Mice were anesthetized under isoflurane using a single animal vaporizer unit (EZ-108SA, E-Z Anesthesia, Palmer, PA). The anesthetized mouse was positioned supine, and 0.5 cm sized dorsal incision was made below the bottom of the rib cage. Subcutaneous tissue was dissected from the underlying muscle, and then approximately 1 cm-

sized incision was made on both sides of spine to approach the peritoneal cavity. The ovarian

fat pad was retracted to identify ovaries. After that, a single ligation was performed around

oviduct, then ovary was removed. The remaining part of the oviduct was returned to the

abdominal cavity. The procedure was repeated on the other side. The muscle layer and skin

incision were closed with simple suture. For sham operations, the ovary was identified and

replaced back into the abdominal cavity.[65]

Prevention of OVX-Induced Osteoporosis. The body weights of female ddY mice were

measured weekly for 5 weeks after OVX. Beginning a week after OVX surgery, mice received

10 mg/kg/d of compounds **1** or **2g**, or alendronate, or 1 or 10 mg/kg/d of compounds **2c** PO

using gavage. Benzylideneacetone derivatives were first dissolved in a minimum amount of

DMSO and diluted to 1 mg/mL of PBS, which were fed 300 µL once daily to OVX mice. The

final concentration of DMSO was 0.5 % (v/v) in PBS in 10 mg/kg/d of benzylideneacetone

derivatives-administered groups and 0.05% (v/v) in 1 mg/kg/d-administered group.

Alendronate was dissolved in PBS containing 0.5% (v/v) DMSO to the final concentration of

1 mg/mL, which was fed 300 µL once daily to OVX mice. PBS containing 0.5 % (v/v) DMSO

as vehicle was fed 300 µL once daily to OVX and sham controls. Test compounds were fed for

4 weeks. Mice were euthanized by heart puncture under isoflurane anesthesia using a single

animal vaporizer unit (EZ-108SA, E-Z Anesthesia), and femur and tibia of each mouse were

obtained.

Histomorphometrical Analysis for the Estimation of Osteoporotic Indices in OVX Mice.

Femur and tibia of each mouse were fixed in 10% neutral buffered formalin (Sigma-Aldrich)

for 2 weeks and subject to Micro-Computed Tomography (CT) analysis using scanner system

(SkyScan1173 Ver. 1.6, Bruker-CT, Kontich, Belgium) to obtain CT and 3-D images in a

scanning condition; source voltage (kV) = 110, source current (µA) = 72, number of rows =

2240, number of columns = 2240, image pixel size (µm) = 13.85, filter = Al 1.0 mm, exposure

(ms) = 500, rotation step (deg) = 0.3, frame averaging = 4. Specimens were wrapped in Parafilm M® (Bemis Company, Inc., Neenah, WI) to keep them from drying during scanning. The CT images of femurs of each mouse in all groups were reconstructed to determine histomorphometrical indices including BMD, BV/TV, Cs.Th, Tb.N, Tb.Th, Tb.Sp, NBV in defect areas, using Nrecon program Ver. 1.7.0.4 (Bruker, Kontich, Belgium) at the following settings; pixel size (µm) = 13.85, angular step (deg) = 0.3, frame averaging = 7, ROI right (pixels) = 2240, ROI reference length = 2240, beam hardening correction (%) = 40, minimum for CS to image conversion = 0.0000, maximum for CS to image conversion = 0.0350. The NRecon reconstruction program was performed using the same applied scan and reconstruction parameters for all specimens. NBV were calculated within the regions of interest.

MTT Assay. Cytotoxicity was assessed by MTT assay as previously described,[35] using an MTT assay kit (Sigma-Aldrich). Briefly, cells were seeded into a 96-well plate at a density of 1×10^5 cells per well in 100 µL of corresponding media and incubated at 37 °C in a 5% CO_2 incubator for 24 h. The culture media were replaced with 100 µL of fresh serum-free media in the presence of varied concentrations of benzylideneacetone derivatives, and cells were incubated for an additional 24 h. Controls were treated with an equal amount of DMSO present in the assay for a 5 mM concentration. Then, media were removed and 100 µL of MTT solution (0.5 mg/mL in media) was added to each well. To measure the proportion of surviving cells, media were replaced with 100 µL of DMSO 2 h after the administration of MTT solution. Absorbance was measured at 570 nm using a spectrophotometric plate reader (Molecular Devices) to determine cellular growth and survival.

Statistical Analysis. Values are expressed as the mean ± SD of three independent experiments, and compared using an unpaired t-test to compare test compound-treated versus

untreated cells using Prism8 (GraphPad, San Diego, CA). P<0.05 was considered statistically significant.

ASSOCIATED CONTENT

Supporting Information

Supporting Information 1

LC spectrum sata for purity validation

Supporting Information 2

^{1}H, ^{13}C NMR spectrum of benzylideneacetone derivatives synthesized *de novo*

Supporting Information 3

Plasma concentration-time curves of compounds **1** and **2c** in male ICR mice

Supporting Information 4

The change of body weight during the administration of benzylideneacetone derivatives to OVX mice

Supporting Information 5

The images of CT scan and 3-D representation of all mice in all experimental groups

Supporting Information 6

Histomorphometrical indices and regenerated bone volume after reconstruction of the CT images of femur of each mouse in all groups using Nrecon Ver. 1.7.0.4 based on the Feldkamp algorithm

Supporting Information 7

Cytotoxicity of Compound **1** and its Natural/Synthetic Derivatives

Supporting Information 8

Molecular Formula Strings Spreadsheet (CSV) and the Associated Biochemical and Biological Data

AUTHOR INFORMATION

Corresponding Author Information

*E-mail: ghpark@korea.ac.kr. Phone: +82 10 5472 4854. Fax: +82 2 923 0480 (G.H.P).

*E-mail: medichem@gbsa.or.kr. Phone: +82 10 2763 1463. Fax: +82 31 888 6979 (J.-M.K).

Author Contributions

#P.T., K.M.H. and L.J.H. contributed equally. The manuscript was contributed by all the authors, who have approved the final version of the manuscript.

CONFLICT OF INTEREST

All authors declare no competing financial interest.

ACKNOWLEDGEMENTS

ABBREVIATIONS

ALP, alkaline phosphatase; BMD, bone mineral density; BMM, bone marrow monocyte/macrophage; BV/TV, percent bone volume; Cs.Th, crossectional thickness; DMEM, Dulbecco's modified Eagle's medium; fluorine, F; LSM, Lymphocyte Separation Medium; M-CSF, macrophage colony-stimulating factor; α-MEM, Minimum Essential Medium Eagle-Alpha Modification; MTT, 3-(4,5-dimethylthiazol-2-yl)-2,5-diphenyltetrazolium bromide; NBV, new bone volume; NFATc1, nuclear factor of activated T-cell cytoplasmic 1; OCN, osteocalcin; OVX, ovariectomy; PTH, parathyroid hormone; SD, standard deviation; RUNX2, Runt-related transcription factor 2; RANK, receptor activator of nuclear factor-kB; RANKL, receptor activator of nuclear factor-kB ligand; Tb.N, trabecular number; Tb.Sp, trabecular separation; Tb.Th, trabecular thickness; TRAP, tartrate-resistant acid phosphatase

REFERENCES

1. Manolagas, S. C.; Jilka, R. L. Bone Marrow, Cytokines, and Bone Remodeling. Emerging Insights into the Pathophysiology of Osteoporosis. *N. Engl. J. Med.* **1995**, *332*, 305-311.

2. Singer, F. R. Bone Quality in Paget's Disease of Bone. *Curr. Osteoporos. Rep.* **2016**, *14*, 39-42.

3. Rodan, G. A.; Martin, T. J. Therapeutic Approaches to Bone Diseases. *Science* **2000**, *289*, 1508-1514.

4. Tamasi, J. A.; Vasilov, A.; Shimizu, E.; Benton, N.; Johnson, J.; Bitel, C. L.; Morrison, N.; Partridge, N. C. Monocyte Chemoattractant Protein-1 Is a Mediator of the Anabolic Action of Parathyroid Hormone on Bone. *J. Bone Miner. Res.* **2013**, *28*, 1975-1986.

5. Schneider, A.; Kalikin, L. M.; Mattos, A. C.; Keller, E. T.; Allen, M. J.; Pienta, K. J.; McCauley, L. K. Bone Turnover Mediates Preferential Localization of Prostate Cancer in the Skeleton. *Endocrinology* **2005**, *146*, 1727-1736.

6. Bruni-Cardoso, A.; Johnson, L. C.; Vessella, R. L.; Peterson, T. E.; Lynch, C. C. Osteoclast-Derived Matrix Metalloproteinase-9 Directly Affects Angiogenesis in the Prostate Tumor-Bone Microenvironment. *Mol. Cancer Res.* **2010**, *8*, 459-470.

7. Shiirevnyamba, A.; Takahashi, T.; Shan, H.; Ogawa, H.; Yano, S.; Kanayama, H.; Izumi, K.; Uehara, H. Enhancement of Osteoclastogenic Activity in Osteolytic Prostate Cancer Cells by Physical Contact with Osteoblasts. *Br. J. Cancer* **2011**, *104*, 505-513.

8. Hung, T. T.; Chan, J.; Russell, P. J.; Power, C. A. Zoledronic Acid Preserves Bone Structure and Increases Survival but Does Not Limit Tumour Incidence in a Prostate Cancer Bone Metastasis Model. *PLoS One* **2011**, *6*, e193889(1-8), DOI: 10.1371/journal.pone.0019389-

9. Marks, S. C. Jr.; Wojtowicz, A.; Szperl, M.; Urbanowska, E.; MacKay, C. A.; Wiktor-Jedrzejczak, W. Administration of Colony Stimulating Factor-1 Corrects Some Macrophage, Dental, and Skeletal Defects in an Osteopetrotic Mutation (toothless, tl) in the Rat. *Bone* **1992**, *13*, 89-93.

10. Anderson, D. M.; Maraskovsky, E.; Billingsley, W. L.; Dougall, W. C.; Tometsko, M. E.; Roux, E. R. A Homologue of the TNF Receptor and its Ligand Enhance T-Cell Growth and Dendritic-Cell Function. *Nature* **1997**, *390*, 175-179.

11. Koga, T.; Inui, M.; Inoue, K.; Kim, S.; Suematsu, A.; Kobayashi, E. Costimulatory Signals Mediated by the ITAM Motif Cooperate with RANKL for Bone Homeostasis. *Nature* **2004**, *428*, 758-763.

12. Mócsai, A.; Humphrey, M. B.; Van Ziffle, J. A.; Hu, Y.; Burghardt, A.; Spusta, S. C. The Immunomodulatory Adapter Proteins DAP12 and Fc Receptor Gamma-Chain (FcRgamma) Regulate Development of Functional Osteoclasts through the Syk Tyrosine Kinase. *Proc. Natl. Acad. Sci. U. S. A.* **2004**, *101*, 6158-6163.

13. Boyce, B. F.; Xiu, Y.; Li, J.; Xing, L.; Yao, Z. NF-kB-Mediated Regulation of Osteoclastogenesis. *Endocrinol. Metab. (Seoul)* **2015**, *30*, 35–44.

14. Asagiri, M.; Sato, K.; Usami, T.; Ochi, S.; Nishina, H.; Yoshida, H. Autoamplification of NFATc1 Expression Determines its Essential Role in Bone Homeostasis. *J. Exp. Med.* **2005**, *202*, 1261-1269.

15. Bonewald, L. F.; Johnson, M. L. Osteocytes, Mechanosensing and Wnt Signaling. *Bone* **2008**, *42*, 606-615.

16. Gong, Y.; Slee, R. B.; Fukai, N.; Rawadi, G.; Roman-Roman, S.; Reginato, A. M.; Wang, H.; Cundy, T.; Glorieux, F. H.; Lev, D.; Zacharin, M.; Oexle, K.; Marcelino, J.; Suwairi, W.; Heeger, S.; Sabatakos, G.; Apte, S.; Adkins, W. N.; Allgrove, J.; Arslan-Kirchner, M.; Batch, J. A.; Beighton, P.; Black, G. C.; Boles, R. G.; Boon, L. M.; Borrone, C.; Brunner, H. G.; Carle, G. F.; Dallapiccola, B.; De Paepe, A.; Floege, B.; Halfhide, M. L.; Hall, B.; Hennekam, R. C.; Hirose, T.; Jans, A.; Jüppner, H.; Kim, C. A.; Keppler-Noreuil, K.; Kohlschuetter, A.; LaCombe, D.; Lambert, M.; Lemyre, E.;

Letteboer, T.; Peltonen, L.; Ramesar, R. S.; Romanengo, M.; Somer, H.; Steichen-Gersdorf, E.; Steinmann, B.; Sullivan, B.; Superti-Furga, A.; Swoboda, W.; Van den Boogaard, M. J.; Van Hul, W.; Vikkula, M.; Votruba, M.; Zabel, B.; Garcia, T.; Baron, R.; Olsen, B. R.; Warman, M. L. Osteoporosis-Pseudoglioma Syndrome Collaborative Group. LDL Receptor-Related Protein 5 (LRP5) Affects Bone Accrual and Eye Development. *Cell* **2001**, *107*, 513-523.

17. Hollinger, J. O.; Onikepe, A. O.; MacKrell, J.; Einhorn, T.; Bradica, G.; Lynch, S.; Hart, C. E. Accelerated Fracture Healing in the Geriatric, Osteoporotic Rat with Recombinant Human Platelet-Derived Growth Factor-BB and an Injectable beta-Tricalcium Phosphate/Collagen Matrix. *J. Orthop. Res.* **2008**, *26*, 83-90.

18. Urist, M. R. Bone: Formation by Autoinduction. *Science* **1965**, *150*, 893-899.

19. Phimphilai, M.; Zhao, Z.; Boules, H.; Roca, H.; Franceschi, R. T. BMP Signaling Is Required for RUNX2-Dependent Induction of the Osteoblast Phenotype. *J. Bone Miner. Res.* **2006**, *21*, 637-646.

20. van Straalen, J. P.; Sanders, E.; Prummel, M. F.; Sanders, G. T. B. Bone-Alkaline Phosphatase as Indicator of Bone Formation. *Clin. Chim. Acta* **1991**, *201*, 27-33.

21. Young, M. F.; Kerr, J. M.; Ibaraki, K.; Heegaard, A. M.; Robey, P. G. Structure, Expression, and Regulation of the Major Noncollagenous Matrix Proteins of Bone. *Clin. Orthop. Relat. Res.* **1992**, *281*, 275-294.

22. Takayanagi, H. Osteoimmunology: Shared Mechanisms and Crosstalk between the Immune and Bone Systems. *Nat. Rev. Immunol.* **2007**, *7*, 292-304.

23. Boyle WJ, Simonet WS, Lacey DL. Osteoclast Differentiation and Activation. *Nature* **2003**, *423*, 337-342.

24. Manolagas SC, Jilka RL. Bone Marrow, Cytokines, and Bone Remodeling. Emerging Insights into the Pathophysiology of Osteoporosis. *N. Engl. J. Med.* **1995**, *332*, 305-311.

25. Hogan, C. M. *Fern: Encyclopedia of Earth*; National Council for Science and the Environment: Washington D.C. USA, 2010.

26. Zhu, X. X.; Li, Y. J.; Yang, L.; Zhang, D.; Chen, Y.; Kmonickova, E.; Weng, X. G.; Yang, Q.; Zídek, Z. Divergent Immunomodulatory Effects of Extracts and Phenolic Compounds from the Fern *Osmunda japonica. Thunb. Chin. J. Integr. Med.* **2013**, *19*, 761-770.

27. McInnes, I. B.; Schett, G. The Pathogenesis of Rheumatoid Arthritis. *N. Engl. J. Med.* **2011**, *365*, 2205-2219.

28. Lyu, H. N.; Lee, D. Y.; Kim, D. H.; Yoo, J. S.; Lee, M. K.; Kim, I. H.; Baek, N. I. Phenolic Compounds from the Fruit Body of *Phellinus linteus* Increase Alkaline Phosphatase (ALP) activity of Human Osteoblast-Like Cells. *Food Sci. Biotechnol.* **2008**, *17*, 1214-1220.

29. Kuriyama, I.; Yuki, N.; Hiroshi, N.; Tetsuya, K.; Toshifumi, T.; Fumio, S.; Hiromi, Y.; Yoshiyuki, M. Inhibitory Effects of Low Molecular Weight Polyphenolics from *Inonotus obliquus* on Human DNA Topoisomerase Activity and Cancer Cell Proliferation. *Mol. Med. Rep.* **2013**, *8*, 35-542.

30. Molina, M.; Reyes-Garcia, M.; Pardo-De-Santayana, M. Local Knowledge and Management of the Royal Fern (*Osmunda regails* L.) in Northern Spain: Implications for Biodiversity Conservation. *Amer. Fern J.* **2009**, *99*, 45-55.

31. Shubhashree, M. N.; Raghavendra, N.; Doddamani, S. H.; Sulochana, B. An Updated Review of Single Herbal Drugs in the Management of Osteoporosis. *IJCAM*. **2018**, *11*, 82-86.

32. Ito, S.; Ohmi, A.; Sakamiya, A.; Yano, T.; Okumura, K.; Nishimura, N.; Kagontani, K. Ginger Hexane Extract Suppresses RANKL-Induced Osteoclast Differentiation. *Biosci. Biotechnol. Biochem.* **2016**, *80*, 779-785.

33. Yogosawa, S.; Yamada, Y.; Yasuda, S.; Sun, Q.; Takizawa, K.; Sakai, T. Dehydrozingerone, a Structural Analogue of Curcumin, Induces Cell-Cycle Arrest at the G2/M Phase and Accumulates Intracellular ROS in HT-29 Human Colon Cancer Cells. *J. Nat. Prod.* **2012**, *75*, 2088-2093.

34. Toutain, P. L.; Bousquet-Mélou A. Plasma Terminal Half-Life. *J. Vet. Pharmacol. Ther*. **2004**, *27*, 427-439.

35. Boyd, M. The NCI Human Tumor Cell Line (60-Cell) Screen. In *Anticancer Drug Development Guide: Preclinical Screening, Clinical Trials and Approval*, 2nd ed.; Teicher, B. A., Andrews, P. A., Eds.; Humana Press Inc.: Totowa, NJ, 2003; pp 41-63.

36. Mosmann, T. Rapid Colorimetric Assay for Cellular Growth and Survival: Application to Proliferation and Cytotoxicity Assays. *J. Immunol. Methods* **1983**, *65*, 55-63.

37. Bergstrom, J. D.; Bostedor, R. G.; Masarachia, P. J; Reszka, A. A; Rodan, G. Alendronate Is a Specific, Nanomolar Inhibitor of Farnesyl Diphosphate Synthase. *Arch. Biochem. Biophys.* **2000**, *373*, 231-241.

38. Zhang, Y.; Chen, X.; Tang, Y.; Lu, Y.; Guo, L.; Zhong, D. Bioequivalence of Generic Alendronate Sodium Tablets (70 mg) to Fosamax® Tablets (70 mg) in Fasting, Healthy Volunteers: A Randomized, Open-Label, Three-Way, Reference-Replicated Crossover Study. *Drug Des. Devel. Ther*. **2017**, *11*, 2109-2119.
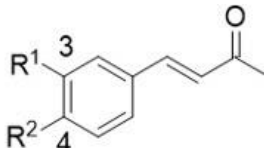
39. Riaz, H.; Godman, B.; Bashir, S.; Hussain, S.; Mahmood, S.; Malik, F.; Waseem, D.; Raza, S. A.; Mahmood, W.; Alamgeer. Comparative Bioavailability Analysis of Oral Alendronate Sodium Formulations in Pakistan. *Acta Pol. Pharm.* **2016**, *73*, 999-1007.

40. Sung, B.; Pandey, M. K.; Nakajima, Y.; Nishida, H.; Konishi, T.; Chaturvedi, M. M.; Aggarwal, B. B. Identification of a Novel Blocker of IkappaBalpha Kinase Activation that Enhances Apoptosis and Inhibits Proliferation and Invasion by Suppressing Nuclear Factor-kappaB. *Mol. Cancer Ther.* **2008**, *7*, 191-201.

41. Takakura, K.; Takatou, S.; Tomiyama, R.; Le, T. M.; Nguyen, D. T.; Nakamura, Y.; Konishi, T.; Matsugo, S.; Hori, O. Inhibition of Nuclear NF-κB p65 Phosphorylation by 3,4-Dihydroxybenzalacetone and Caffeic Acid Phenethyl Ester. *J. Pharmacol. Sci.* **2018**, *137*, 248-255.

42. Park, J. H.; Lee, N. K.; Lee, S. Y. Current Understanding of RANK Signaling in Osteoclast Differentiation and Maturation. *Mol. Cells* **2017**, *40*, 706-713.

43. Capuzzi, S. J; Muratov, E. N.; Tropsha, A. Phantom PAINS: Problems with the Utility of Alerts for Pan-Assay Interference Compounds. *J. Chem. Inf. Model* **2017**, *57*, 417-427.

44. Baell, J. B. Feeling Nature's PAINS: Natural Products, Natural Product Drugs, and Pan Assay Interference Compounds (PAINS). *J. Nat. Prod.* **2016**, *79*, 616-628.

45. Jackson, P. A.; Widen, J. C.; Harki, D. A.; Brummond, K. M. Covalent Modifiers: A Chemical Perspective on the Reactivity of α,β-Unsaturated Carbonyls with Thiols via Hetero-Michael Addition Reactions. *J. Med. Chem.* **2017**, *60*, 839-885.

46. Kohler, J.; Schuler, M. Afatinib, Erlotinib and Gefitinib in the First-Line Therapy of EGFR Mutation-Positive Lung Adenocarcinoma: A Review. Onkologie **2013**, *36*, 510-518.

47. Serafimova, I. M.; Pufall, M. A.; Krishnan, S.; Duda, K.; Cohen, M. S.; Maglathlin, R. L.; McFarland, J. M.; Miller, R. M.; Frodin, M.; Taunton, J. Reversible Targeting of Noncatalytic Cysteines with Chemically Tuned Electrophiles. *Nat. Chem. Biol*. **2012**, *8*, 471-476.

48. Miller, R. M.; Paavilainen, V. O.; Krishnan, S.; Serafimova, I.; Taunton, J. Electrophilic Fragment-Based Design of Reversible Covalent Kinase Inhibitors. *J. Am. Chem. Soc*. **2013**, *135*, 5298-5301.

49. Maucher, I. V.; Rühl, M.; Kretschmer, S. B. M.; Hofmann, B.; Kühn, B.; Fettel, J.; Vogel, A.; Flügel, K. T.; Manolikakes, G.; Hellmuth, N.; Häfner, A-K.; Golghalyani, V.; Ball, A-K.; Piesche, M.; Matrone, C.; Geisslinger, G.; Parnham, M. J.; Karas, M.; Steinhilber, D.; Roos, J.; Maier, T. J. Michael Acceptor Containing Drugs Are a Novel Class of 5-Lipoxygenase Inhibitor Targeting the Surface Cysteines C416 and C418. *Biochem. Pharmacol*. **2017**, *125*, 55-74.

50. Nakamura, T.; Imai, Y.; Matsumoto, T.; Sato, S.; Takeuchi, K.; Igarashi, K.; Harada, Y.; Azuma, Y.; Krust, A.; Yamamoto, Y.; Nishina, H.; Takeda, S.; Takayanagi, H.; Metzger, D.; Kanno, J.; Takaoka, K.; Martin, T. J.; Chambon, P.; Kato, S. Estrogen Prevents Bone Loss via Estrogen Receptor α and Induction of Fas Ligand in Osteoclasts. *Cell* **2007**, *130*, 811-823.

51. Smith, M. R.; Saad, F.; Coleman, R.; Shore, N.; Fizazi, K.; Tombal, B.; Miller, K.; Sieber, P.; Karsh, L.; Damião, R.; Tammela, T. L.; Egerdie, B.; Van Poppel, H.; Chin, J.; Morote, J.; Gómez-Veiga, F.; Borkowski, T.; Ye, Z.; Kupic, A.; Dansey, R.; Goessl, C. Denosumab and Bone-Metastasis-Free Survival in Men with Castration-Resistant Prostate Cancer: Results of a Phase 3, Randomised, Placebo-Controlled Trial. *Lancet* **2012**, *379*, 39-46.

52. Sun, K.; Liu, J. M.; Sun, H. X.; Lu, N.; Ning, G. Bisphosphonate Treatment and Risk of Esophageal Cancer: a Meta-Analysis of Observational Studies. *Osteoporos. Int.* **2013**, *24*, 279-286.

53. Ripamonti, C. I.; Maniezzo, M.; Campa, T.; Fagnoni, E.; Brunelli, C.; Saibene, G.; Bareggi, C.; Ascani, L.; Cislaghi, E. Decreased Occurrence of Osteonecrosis of the Jaw after Implementation of Dental Preventive Measures in Solid Tumour Patients with Bone Metastases Treated with Bisphosphonates. The Experience of the National Cancer Institute of Milan. *Ann. Oncol.* **2009**, *20*, 137-145.

54. Khosla, S. Increasing Options for the Treatment of Osteoporosis. *N. Engl. J. Med.* **2009**, *361*, 818-820.

55. Rizzoli, R.; Reginster, J. Y.; Boonen, S.; Bréart, G. R.; Diez-Perez, A.; Felsenberg, D.; Kaufman, J. M.; Kanis, J. A.; Cooper, C. Adverse Reactions and Drug-Drug Interactions in the Management of Women with Postmenopausal Osteoporosis. *Calcif. Tissue Int.* **2011**, *89*, 91-104.

56. Weilbaecher, K. N.; Guise, T. A.; McCauley, L. K. Cancer to Bone: a Fatal Attraction. *Nat. Rev. Cancer* **2011**, *11*, 411-425.

57. Zhuang, J.; Zhang, J.; Lwin, S. T.; Edwards, J. R.; Edwards, C. M.; Mundy, G. R.; Yang, X. Osteoclasts in Multiple Myeloma Are Derived from Gr-1+ CD11b+ Myeloid-Derived Suppressor Cells. *PLoS One* **2012**, *7*, e48871(1-11), doi.org/10.1371/journal.pone.0048871.

58. El-Amm, J.; Freeman, A.; Patel, N.; Aragon-Ching, J. B. Bone-Targeted Therapies in Metastatic Castration-Resistant Prostate Cancer: Evolving Paradigms. *Prostate Cancer* **2013**, *2013*, Article ID 210686, doi.org/10.1155/2013/210686.

59. Wirth, M.; Tammela, T.; Cicalese, V.; Gomez Veiga, F.; Delaere, K.; Miller, K.; Tubaro, A.; Schulze, M.; Debruyne, F.; Huland, H.; Patel, A.; Lecouvet, F.; Caris, C.; Witjes, W. Prevention of Bone Metastases in Patients with High-Risk Nonmetastatic Prostate Cancer Treated with Zoledronic Acid: Efficacy and Safety Results of the Zometa European Study (ZEUS). *Eur. Urol.* **2015**, *67*, 482-491.

60. Tatsuzaki, J.; Kenneth, F. B.; Kyoko, N. G.; Seiko, N.; Hideji, I.; Lee, K. H. Dehydrozingerone, Chalcone, and Isoeugenol Analogues as *In Vitro* Anticancer Agent. *J. Nat. Prod.* **2006**, *69*, 1445-1449.

61. Wasserman, A. M. Diagnosis and Management of Rheumatoid Arthritis. *Am. Fam. Physician* **2011**, *84*, 1245-1252.

62. Gurt, I.; Artsi, H.; Cohen-Kfir, E.; Hamdani, G.; Ben-Shalom, G.; Feinstein, B.; El-Haj, M.; Dresner-Pollak, R. The Sirt1 Activators SRT2183 and SRT3025 Inhibit RANKL-Induced Osteoclastogenesis in Bone Marrow-Derived Macrophages and Down-Regulate Sirt3 in Sirt1 Null Cells. *PLoS One* **2015**, *10*, e0134391(1-14), doi.org/10.1371/journal.pone.0134391.

63. Delaissé, J. M.; Andersen, T. L.; Engsig, M. T.; Henriksen, K.; Troen, T.; Blavier, L. Matrix Metalloproteinases (MMP) and Cathepsin K Contribute Differently to Osteoclastic Activities. *Microsc. Res. Tech.* **2003**, *61*, 504-513.

64. Schiller, P. C.; D'Ippolito, G.; Roos, B. A.; Howard, G. A. Anabolic or Catabolic Responses of MC3T3-E1 Osteoblastic Cells to Parathyroid Hormone Depend on Time and Duration of Treatment. *J. Bone Miner. Res*. **1999**, *14*, 1504-1512.

65. Idris, A. I. Ovariectomy/Orchidectomy in Rodents. In *Bone Research Protocols, Methods in Molecular Biology*, Vol. 816; Helfrich M. H., Ralston S. H., Eds.; Humana Press: New Jersey, 2011; pp 545-548.

1
2
3
4
5
6
7
8
9
10
11
12
13
14
15
16
17
18
19
20
21
22
23
24
25
26
27
28
29
30
31
32
33
34
35
36
37
38
39
40
41
42
43
44
45
46
47
48
49
50
51
52
53
54
55
56
57
58
59
60

Table of Contents Graphic

R^1 = OMe, R^2 = OH, Compound 2g
R^1 = OH, R^2 = OMe, Compound 2c
R^1 = OH, R^2 = OH, Compound 1

Application

Osteoporosis
Bone metastasis
Rheumatoid arthritis

	Osteoclastogenesis IC_{50} (µM) on TRAP assay Monocyte/macrophage	Osteoblastogenesis % Activation of ALP (50 µM) MC3T3-E1 preosteoblast	Cytotoxicity LD_{50} (µM) Macrophage
Compound 2g	7.5 ± 0.5	600 ± 70	>5,000
Compound 2c	0.11 ± 0.02	180 ± 20	>5,000
Compound 1	7.8 ± 2	280 ± 60	500 ± 40
Alendronate	3.7 ± 1		
PTH-related peptide (1 µM)		140 ± 20	